



# Analysis of thermochemical properties and phase stability in the zirconium–carbon system

A. Fernández Guillermet

*Consejo Nacional de Investigaciones Científicas y Técnicas, Comisión Nacional de Energía Atómica, Centro Atómico Bariloche, 8400 Bariloche, Argentina*

Received 12 May 1994

## Abstract

Experimental information on the thermochemical properties and the phase equilibria involving the condensed phases of the Zr–C system has been analysed using phenomenological models for Gibbs energy. The solid solutions of carbon in the h.c.p. and b.c.c. phases of Zr and the non-stoichiometric NaCl-type structure  $ZrC_x$  carbide are treated by using the compound energy model (CEM) for interstitial phases. The liquid phase is treated by using a substitutional solution model and the Redlich–Kister formalism for excess Gibbs energies. The parameters in the models are determined by computerized optimization of selected experimental data. The metastable carbides  $ZrC_{0.5}$  and  $ZrC_3$ , that are involved in the CEM for the interstitial solutions of C in h.c.p. and b.c.c. Zr respectively, are described using estimated values for the entropy and enthalpy of formation. These estimates are based on the regular behaviour of the vibrational entropy and other cohesive properties which have been established in recent studies on transition metal compounds. A thermodynamic description is obtained which is used to construct, by calculation, the Zr–C phase diagram. Detailed comparisons are presented between calculations and experimental data of various kinds. The enthalpy of formation values predicted by Miedema and coworkers are also confronted with the present results.

*Keywords:* Thermochemical properties; Phase stability; Zirconium–carbon system; Enthalpy of formation

## 1. Introduction

The thermodynamic properties and the phase diagram of transition metal systems are a subject of continuous interest in basic materials science. Thermodynamic quantities provide a kind of information on the cohesive properties of alloys and compounds which is well adapted for systematic studies of regularities and trends. In addition, binary thermodynamic information forms the basis of a powerful theoretical approach to phase stability in multicomponent alloy systems which is usually known as the CALPHAD approach [1] (i.e. the computer coupling of phase diagrams and thermochemistry). In particular, the compounds formed by a transition metal (Me) with C have been the subject of extensive research, and there is reasonably accurate experimental information on the phase diagram of several Me–C systems [2]. By combining this information with available measurements of the so-called thermochemical properties, it has been possible to perform detailed evaluations of the Gibbs energy functions of the various phases in

Me–C systems formed by 3d transition metals (i.e. Me  $\equiv$  Ti [3], V [4], Cr [5], Mn [6], Fe [7], Co [8] and Ni [9]), the 4d transition metals (i.e. Me  $\equiv$  Nb [10] and Mo [11]) and the 5d transition metals (i.e. Me  $\equiv$  W [12]). The Gibbs energy functions obtained in this way have been used as a basis for recent descriptions of higher-order systems, e.g. the Fe–Cr–Mo–C [13], Fe–V–Mn–C [14], Fe–Cr–Mo–W–C [15] and Fe–Co–Ni–W–C [16] systems. In addition, assessed thermochemical values have been included in systematic studies of the bonding properties of binary carbides formed by the 3d [17,18], 4d [19] and 5d [20] transition metals. In view of the considerable theoretical and practical importance of the thermodynamic information on binary Me–C systems, we shall now focus on the Zr–C system.

Because of the technical importance of the Zr carbide as a hard, high melting compound, the thermodynamic properties of the Zr–C system have been studied on several occasions. The experimental information on the phase diagram has been compiled by Hayes [21], Hansen

and Anderko [22], Elliott [23], Storms [24], Shunk [25], Hultgren et al. [26] and Kubaschewski-von Goldbeck [27] and by Okamoto [28], who presented the most recent version of the Zr–C phase diagram. The thermochemical data available, which mainly concern the Zr carbide phase, have been compiled by Kubaschewski and Catterall [29], Storms [24], Schick [30], Hultgren et al. [26] and Alcock et al. [31], and by Chase et al. in the JANAF Thermochemical Tables [32]. Some thermodynamic analyses of the data have also been reported. The thermodynamics of the Zr carbide phase was treated by De Poorter [33], Hoch [34] and others [35] in terms of models derived from the statistical mechanics of interstitial phases, whereas Kaufman and Sarney [36] and Chang [37] used the Schottky–Wagner model. Moreover, Kaufman and Clougherty [38] reported a calculation of the Zr–C phase diagram which reproduced reasonably well the main features of the phase diagram recommended by Hansen and Anderko [22].

More recently, there have been studies of the thermodynamic properties of the Zr–C system. The properties of the h.c.p., b.c.c. and liquid phase of Zr have been assessed by Fernández Guillermet [39], and Saunders et al. [40] have estimated the properties of the metastable f.c.c. Zr. Furthermore, Gustafson [41] has presented a thermodynamic description of solid and liquid carbon. In addition a number of studies of the thermochemical properties (e.g. enthalpy of formation, heat content, heat capacity, activity of Zr) and the phase diagram have been reported since the reviews by Kubaschewski-von Goldbeck [27] and Alcock et al. [31], which makes it appropriate to perform a new analysis of the thermochemistry and phase equilibrium in the Zr–C system. Such an analysis is performed in the present study by applying a model for the Gibbs energy function of the non-stoichiometric so-called [42–44] interstitial phases, i.e. the compound energy model (CEM) [45,46]. The CEM is phenomenological and contains parameters which are to be determined by analysing experimental data. These parameters are of two kinds. One group of parameters represents the Gibbs energy of stoichiometric compounds which are stable or metastable in the system, and the other group describes the deviations from the ideal behaviour in the non-stoichiometric interstitial phases. In this work, these parameters are determined by combining the analysis of experimental information using a computer optimization technique with estimation of thermodynamic properties for metastable compounds, which is based on the regular behaviour of the bonding properties and vibrational entropy of transition metal carbides [17,18].

The outline of the paper is as follows. In Section 2 we present the models for the Gibbs energy of the various phases in the system, and in Section 3 we explain

the procedure for evaluating the parameters in the models. Section 4 is devoted to the experimental data used in the evaluation and Section 5 to the estimation of thermodynamic quantities for metastable compounds. In Section 6 we present and discuss the results, and in Section 7 we summarize the work and present our conclusions.

## 2. Thermodynamic modelling

### 2.1. Phases and structures

There is general agreement on the existence of five stable condensed phases in the Zr–C phase diagram [21–28]. These phases, which will be dealt with in the present study, are the following:

- (1) the Zr-rich solid solution of C in h.c.p. (hP2) Zr, or  $\alpha$  phase;
- (2) the Zr-rich solid solution of C in b.c.c. (cI2) Zr, or  $\beta$  phase;
- (3) the (cF8) NaCl-type structure non-stoichiometric carbide  $ZrC_x$ , with  $x \leq 1$ , which will be denoted in this work as the  $\gamma$  phase;
- (4) the hexagonal (hP4) graphite modification of carbon;
- (5) the liquid phase.

### 2.2. Gibbs energy of interstitial phases

The solid solution of C in h.c.p. (hP2) and b.c.c. (cI2) Zr may be considered as derived from the stable h.c.p. and b.c.c. structures of Zr by filling up only a small fraction of the octahedral interstitial sites with C atoms, whereas the non-stoichiometric  $ZrC_x$  carbide may be considered as derived from the metastable f.c.c. (cF4) structure of Zr by filling up an appreciable amount of the octahedral interstitial sites with C atoms. Following Hägg [42] and others [43,44] we shall refer to them as interstitial phases. The Gibbs energy of these phases was described using a two-sublattice [46] version of the CEM [45]. Zr atoms were assumed to occupy the first sublattice whereas C atoms and vacant (Va) interstitial sites were assumed to substitute for each other on the second. Accordingly, the h.c.p. ( $\alpha$ ), b.c.c. ( $\beta$ ) and  $ZrC_x$  ( $\gamma$ ) phases of the Zr–C system were represented by the two-sublattice model  $(Zr)_1(C, Va)_c$ , and the Gibbs energy  $G_m^\phi$  per mole of formula units was represented by the expression

$$G_m^\phi = y_C^0 G_{Zr:C}^\phi + y_{Va}^0 G_{Zr:Va}^\phi + cRT(y_C \ln y_C + y_{Va} \ln y_{Va}) + {}^E G_m^\phi \quad (1)$$

The variable  $y_i$  ( $i = C, Va$ ), which has been referred to as the site fraction [47] of  $i$  measures the fraction of the available sites which is occupied by the component

*i.* The parameter  $c$  represents the number of interstitial sites per metallic atom. The quantity  ${}^0G_{\text{Zr,Va}}^\phi$  is the Gibbs energy of Zr with the structure  $\phi$  ( $\phi = \alpha, \beta, \gamma$ ), and  ${}^0G_{\text{Zr,C}}^\phi$  represents the Gibbs energy of a state where all the interstitial sites are filled with C atoms. All  ${}^0G^\phi$  values were referred to the enthalpy  $H$  of a special standard state recommended by the Scientific Group Thermodata Europe organization [48]. This state, the stable element reference (SER) state, is defined as the stable state of the elements at 298.15 K and  $10^5$  Pa.

The last term in Eq. (1), which represents the excess Gibbs energy of the  $\phi$  phase, was described by using the subregular approximation of the Redlich–Kister [49] phenomenological power series, i.e.

$${}^E G_m^\phi = y_C y_{\text{Va}} [{}^0 L_{\text{Zr,C,Va}}^\phi + {}^1 L_{\text{Zr,C,Va}}^\phi (y_C - y_{\text{Va}})] \quad (2)$$

In Eqs. (1) and (2) the comma separates components that interact in the same sublattice and the colon separates components in different sublattices. The composition-independent parameters  $L^\phi$  in Eq. (2) account phenomenologically for the interaction between C atoms and vacant interstitial sites. They were allowed to vary with temperature according to

$${}^0 L_{\text{Zr,C}}^\phi = {}^0 A_{\text{Zr,C,Va}}^\phi + B_{\text{Zr,C,Va}}^\phi T + C_{\text{Zr,C,Va}}^\phi T \ln T + D_{\text{Zr,C,Va}}^\phi T^2 \quad (3)$$

$${}^1 L_{\text{Zr,C}}^\phi = {}^1 A_{\text{Zr,C,Va}}^\phi + B^{\phi\text{Zr,C,Va}} T + C_{\text{Zr,C,Va}}^\phi T \ln T + D_{\text{Zr,C,Va}}^\phi T^2 \quad (4)$$

In the treatment of the interstitial phase  $\gamma$  (Section 2.3) the five coefficients in Eqs. (3) and (4) were determined from experimental data (Section 3). The remaining interstitial phases were treated using the regular-solution approximation, by setting the parameters  ${}^1 L^\phi$ ,  $C_{\text{Zr,C,Va}}^\phi$  and  $D_{\text{Zr,C,Va}}^\phi$  equal to zero. The various choices about  $L$  parameters made in the present work depend on the amount of information available. They represent a compromise between an accurate description of the selected data and the desire of working with a few, statistically significant parameters.

### 2.3. The $\gamma$ interstitial phase and the stoichiometric ZrC (cF8) carbide

The  $\gamma$  carbide phase has  $c=1$  and it is written as  $(\text{Zr})_1(\text{C, Va})_1$  according to the two-sublattice model [46]. In this case Eq. (1) contains the parameter  ${}^0G_{\text{Zr,Va}}^\gamma$ , the Gibbs energy of f.c.c. Zr, and  ${}^0G_{\text{Zr,C}}^\gamma$ , the Gibbs energy of the stoichiometric (cF8) NaCl-type structure carbide ZrC. Information about the function  ${}^0G_{\text{Zr,Va}}^\gamma - H_{\text{Zr}}^{\text{SER}}$  (Section 2.2), was taken from Refs. [39] and [40], whereas the quantity  ${}^0G_{\text{Zr,C}}^\gamma$  was referred to the enthalpy of the elements Zr and C in their reference states as

$${}^0G_{\text{Zr,C}}^\gamma - H_{\text{Zr}}^{\text{SER}} - H_{\text{C}}^{\text{SER}} = \Delta^0 G_m^\gamma(T) \quad (5)$$

and the temperature-dependent function  $\Delta^0 G_m^\gamma(T)$  was expressed as

$$\Delta^0 G_m^\gamma(T) = a + bT + cT \ln T + dT^2 + eT^3 + fT^{-1} + gT^{-3} \quad (6)$$

with coefficients determined as explained in Section 3.

### 2.4. Interstitial solution based on h.c.p. Zr and the ZrC<sub>0.5</sub> (hP3) carbide

The arrangement of metallic atoms in h.c.p. Zr yields one octahedral interstitial site per atom. However, by adopting the approximation used in previous treatments of the solubility of C and N in the h.c.p. phase of Ti [3,50] and Co [8,51] it was assumed that two neighbouring interstitial sites in the  $c$  direction are never simultaneously occupied. This phase was thus treated with the two-sublattice model  $(\text{Zr})_1(\text{C, Va})_{0.5}$ . The parameter  ${}^0G_{\text{Zr,Va}}^\alpha$  represents the Gibbs energy of h.c.p. Zr. It was taken from the study by Fernández Guillermet [39].  ${}^0G_{\text{Zr,C}}^\alpha$  represents the Gibbs energy of the ZrC<sub>0.5</sub> carbide based on h.c.p. Zr, which is metastable in the Zr–C system. This quantity was referred to the enthalpy of the elements as in Eq. (5), with the corresponding  $\Delta^0 G_m^\alpha(T)$  function represented as in Eq. (6).

### 2.5. Interstitial solution based on b.c.c. Zr and the ZrC<sub>3</sub> carbide

For the interstitial solution of C in b.c.c. Zr, called the  $\beta$  phase, the two-sublattice [46] form of the CEM [45] is  $(\text{Zr})_1(\text{C, Va})_3$ . In that case Eq. (1) involves the parameter  ${}^0G_{\text{Zr,Va}}^\beta$ , i.e. the Gibbs energy of b.c.c. Zr [39], and  ${}^0G_{\text{Zr,C}}^\beta$ , which refers to the carbide in which all octahedral interstitial sites of the b.c.c. structure of Zr are filled up with C atoms. That carbide has the formula ZrC<sub>3</sub> and is metastable in the Zr–C system.  ${}^0G_{\text{Zr,C}}^\beta$  was referred to the enthalpy of the elements in their reference states (Eq. (5)), and the  $\Delta^0 G_m^\beta(T)$  function was described as in Eq. (6).

### 2.6. Graphite

The Gibbs energy of graphite was described by using the  ${}^0G_{\text{C}}^{\text{graph}} - H_{\text{C}}^{\text{SER}}$  function assessed by Gustafson [41].

### 2.7. Liquid phase

The Gibbs energy of the liquid phase was described by adopting a substitutional solution model as follows:

$$G_m^{\text{liq}} = x_{\text{C}} {}^0G_{\text{C}}^{\text{liq}} + x_{\text{Zr}} {}^0G_{\text{Zr}}^{\text{liq}} + RT(x_{\text{C}} \ln x_{\text{C}} + x_{\text{Zr}} \ln x_{\text{Zr}}) + {}^E G_m^{\text{liq}} \quad (7)$$

where  $x_i$  ( $i = \text{Zr}, \text{C}$ ) is the atomic fraction of the component  $i$  in the liquid phase. The quantities  ${}^0G_{\text{C}}^{\text{liq}}$  and  ${}^0G_{\text{Zr}}^{\text{liq}}$  were taken from Refs. [41] and [39] respectively, and the excess Gibbs energy term  ${}^E G_{\text{m}}^{\text{liq}}$  was treated by using the Redlich–Kister [49] phenomenological power series, i.e.

$${}^E G_{\text{m}}^{\text{liq}} = x_{\text{C}} x_{\text{Zr}} [{}^0 L_{\text{C}, \text{Zr}}^{\text{liq}} + {}^1 L_{\text{C}, \text{Zr}}^{\text{liq}} (x_{\text{C}} - x_{\text{Zr}}) + {}^2 L_{\text{C}, \text{Zr}}^{\text{liq}} (x_{\text{C}} - x_{\text{Zr}})^2] \quad (8)$$

In Eq. (8)  ${}^0 L^{\text{liq}}$  was allowed to vary linearly with temperature, but  ${}^1 L^{\text{liq}}$  and  ${}^2 L^{\text{liq}}$  were treated as constants. These choices, as well as the number of terms in Eq. (8), were arrived at by trial and error during the work.

### 3. Evaluation of thermodynamic parameters

Ten Gibbs energy parameters were determined in the present evaluation. Among them,  $\Delta^0 G_{\text{m}}^{\gamma}(T)$ ,  $\Delta^0 G_{\text{m}}^{\alpha}(T)$  and  $\Delta^0 G_{\text{m}}^{\beta}(T)$  describe the Gibbs energy of formation of the stoichiometric ZrC carbide and the metastable  $\text{ZrC}_{0.5}$  and  $\text{ZrC}_3$  carbides respectively. The remaining parameters  ${}^0 L^{\text{liq}}$ ,  ${}^1 L^{\text{liq}}$ ,  ${}^2 L^{\text{liq}}$ ,  ${}^0 L^{\gamma}$ ,  ${}^1 L^{\gamma}$ ,  ${}^0 L^{\alpha}$  and  ${}^0 L^{\beta}$  account phenomenologically for the deviations from ideality in the condensed liquid,  $\gamma$ ,  $\alpha$  and  $\beta$  phases. The evaluation procedure was as follows. All parameters describing the Gibbs energy of formation of ZrC were determined by analysing experimental data on the thermochemical properties and equilibrium boundaries of the non-stoichiometric  $\text{ZrC}_x$  carbide. Lacking direct measurements, the parameters  $b^{\phi}$ ,  $c^{\phi}$ ,  $d^{\phi}$ ,  $e^{\phi}$ ,  $f^{\phi}$  and  $g^{\phi}$  of Eq. (6) (with  $\phi = \alpha, \beta$ ), which describe the temperature dependence of  $G_{\text{m}}$  for the metastable  $\text{ZrC}_{0.5}$  and  $\text{ZrC}_3$  carbides, were determined by fitting Eq. (6) to estimated entropy values at various temperatures. Next the  $a^{\phi}$  and  $L$  parameters were determined by searching for the best fit to selected pieces of experimental information on the phase diagram and thermochemical properties. The fits to the experimental and estimated input values were made by using a computer optimization program [52]. The program optimizes the model parameters that are set free to vary, and it automatically finds the optimum set of parameters by minimizing the square sum of the differences between experimental and calculated values while giving each piece of information a certain weight. The weights were chosen by personal judgment and changed by trial and error during the work, until most of the input information was accounted for within the expected uncertainty limits. This iterative procedure will be referred to in the following as optimization.

## 4. Review and selection of thermodynamic information

### 4.1. Phase diagram information

#### 4.1.1. The liquid– $\gamma$ +liquid equilibrium

Information about the melting point of the Zr carbide is available from the early work by Friederich and Sitting [53] and Agte and Alterthum [54]. More recent values are given by Glaser [55], Brownlee [56], Farr [57], Paderno [58], Sara [59], Rudy et al. [60], Rudy and Progulski [61], Rudy [62] and Zotov and Kotelnikov [63]. The present work was based on the results by Sara [59] and Rudy and coworkers [60–62] after correcting them to the IPTS68 temperature scale. Additional data on the position of the liquid– $\gamma$ +liquid equilibrium boundary were taken from the work by Sara [59] and by Adelsberg et al. [64].

#### 4.1.2. The $\gamma$ +liquid+graphite equilibrium

The  $\gamma$ +liquid+graphite equilibrium has been studied experimentally by Agte and Moers [65], Chiotti and Weiner [66], Portnoi et al. [67], Farr [57], Wallace et al. [68], Sara [59], Rudy et al. [60,62], Adelsberg et al. [69], and Zotov and Kotelnikov [63]. A three-phase equilibrium temperature in agreement with Rudy and coworkers [60–62] and Zotov and Kotelnikov [63] and the composition of the  $\gamma$  phase reported by Sara [59] were selected. The composition of the liquid phase in equilibrium with  $\gamma$  and graphite is not well known, and a value reported by Sara [59] from metallographic observation was adopted.

#### 4.1.3. The $\beta$ +liquid+ $\gamma$ equilibrium

The b.c.c.+liquid+ $\gamma$  three-phase equilibrium temperature has been studied experimentally by Benesovsky and Rudy [70], Farr [57], Rudy [60,62], and Bhatt et al. [71]. The result due to Bhatt et al. [71], which is the most recent, was selected in the present work. The composition of the  $\gamma$  phase in equilibrium with b.c.c. and liquid was taken from the results by Rudy [62] and Storms and Griffin [72]. Accurate information on the composition of the b.c.c. and liquid phase at the three-phase equilibrium temperature is lacking, and previous assessments have been based on some indications [73] that the solubility of C is very low. Estimated solubility values in agreement with Storms [24], Kubaschewski-von Goldbeck [27], and Sara [59] were adopted, but they were given rather low weights in the optimization procedure.

#### 4.1.4. The $\gamma$ – $\gamma$ + $\beta$ and $\gamma$ – $\gamma$ +graphite equilibrium boundaries

Experimental information on the position of the  $\gamma$ – $\gamma$ + $\beta$  and  $\gamma$ – $\gamma$ +graphite equilibrium boundaries was

taken from the works by Farr [57], Rudy et al. [60,62], and Storms and Griffin [72].

#### 4.1.5. The $\alpha + \beta + \gamma$ equilibrium

The temperature of the  $\alpha + \beta + \gamma$  three-phase equilibrium has been reported by Sara [59] and by Rudy et al. [60,62]. The value of Sara [59] was preferred. The compositions of the  $\alpha$  and  $\beta$  phase in equilibrium with  $\gamma$  are not known, and previous versions of the Zr–C phase diagram [23–25,27,28] have assumed that the solubility of C in solid Zr is negligible. Solubility values in agreement with previous estimates for C in solid Zr [73,74] were included in the present optimization.

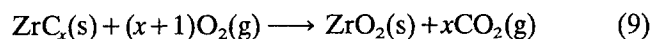
#### 4.1.6. The $\gamma - \gamma + \alpha$ equilibrium

The position of the  $\gamma - \gamma + \alpha$  equilibrium boundary has not been determined experimentally.

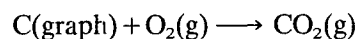
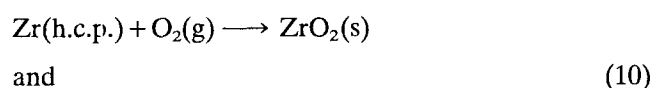
### 4.2. Thermochemical information

#### 4.2.1. Enthalpy of formation of Zr carbides

Values for the enthalpy of formation of the Zr carbides have been obtained from calorimetric measurements and from studies of the vaporization behaviour of the  $ZrC_x$  phase. The calorimetric values are obtained by combining measurements of the so-called heat of combustion of  $ZrC_x$ , i.e. the enthalpy change for the reaction



with values for the enthalpy of formation of  $ZrO_2(s)$  and  $CO_2(g)$  according to the reactions



at 298.15 K and 101325 Pa. The enthalpy of formation of  $ZrO_2(s)$  has been determined by Humphrey [75] and by Huber et al. [76]. The results by Huber et al. [76], which are the most recent, were preferred in the present work. Heat of combustion measurements have been reported by Mah and Boyle [77], Mah [78], and Baker et al. [79]. The results from Baker et al. [79] were combined with the enthalpy of formation of  $ZrO_2$  selected above [76], and the enthalpy of formation of  $CO_2(g)$  recommended in the JANAF Tables [32] and by Kubaschewski and Alcock [80], and values for the enthalpy of formation of  $ZrC_{0.63}$ ,  $ZrC_{0.77}$ ,  $ZrC_{0.84}$  and  $ZrC_{0.98}$  were obtained. They were included in the optimization procedure. The enthalpy of formation values for Zr carbides recommended by Kornilov et al. [81] and those obtained by Maslov et al. [82] by applying a high temperature method were considered but not used in the present study.

Additional information on the enthalpy of formation of Zr carbides has previously been derived from studies of the vaporization behaviour of the  $ZrC_x$  phase, and the reader is referred to Storms [24] and Alcock et al. [31] for a review of the early work. The enthalpy of formation values obtained by Pollock [83] and by Coffman et al. [84] were considered but used only for comparisons with the present results.

#### 4.2.2. Low temperature heat capacity and entropy of Zr carbides

The heat capacity of  $ZrC_{0.96}$  between 5 and 350 K has been determined by Westrum and Feick [85]. Their heat capacity and entropy values corresponding to temperatures between 150 K and 298.15 K were included in the optimization procedure.

#### 4.2.3. Heat content of Zr carbides

Values for the heat content of  $ZrC_x$  have been reported by Neel et al. [86], Mezaki and coworkers [87,88], Levinson [89], Bolgar et al. [90], Kantor and Fomichev [91], Turchanin and Fesenko [92–94], Fesenko et al. [95], Turchanin [96,97], and Sheindlin et al. [98]. The high temperature heat contents reported by Bolgar et al. [90] for  $ZrC_{0.96}$ , by Kantor and Fomichev [91] for  $ZrC$ , and by Turchanin and Fesenko [92] for  $ZrC_{0.69}$ ,  $ZrC_{0.76}$  and  $ZrC_{0.99}$  were included in the optimization procedure.

#### 4.2.4. High temperature heat capacity of Zr carbides

Heat capacity data for  $ZrC_x$  at high temperatures have been reported by Valentine et al. [99], McDonald et al. [100], Mebed et al. [101], Kolesnichenko and Pustogarov [102] and Petrova and Chekhovskoi [103]. Since there are significant discrepancies between the results of the various authors, these heat capacity values were not used in the evaluation of thermodynamic parameters.

#### 4.2.5. Composition dependence of the activity of C and Zr in $\gamma$

The Zr activity in the  $\gamma$  phase was determined by Storms and Griffin [72] at 2103 K (IPTS68), and by Andrievskii et al. [104] at 2500 K. Ten activity values covering compositions between  $ZrC_{0.64}$  and  $ZrC_{0.99}$  were selected from the work by Storms and Griffin [72] and six values, covering the composition range between  $ZrC_{0.63}$  and  $ZrC_{0.95}$  were selected from Andrievskii et al. [104]. They were used in the evaluation of thermodynamic parameters.

#### 4.2.6. Temperature dependence of the Zr activity at the $\gamma + \text{graphite}$ equilibrium

Storms and Griffin [72] determined the activity of Zr in two-phase mixtures of  $\gamma + \text{graphite}$ . Eleven activity values, covering temperatures between 2138 and 2509

K (IPPTS68), were selected from their work and included in the optimization.

## 5. Estimation of entropies and enthalpies of formation for metastable zirconium carbides

Among the Gibbs energy functions to be determined in the present work,  ${}^0G_{\text{Zr,C}}^{\alpha}$  and  ${}^0G_{\text{Zr,C}}^{\beta}$  represent the Gibbs energy of the metastable  $\text{ZrC}_{0.5}$  and  $\text{ZrC}_3$  carbides. Lacking enough experimental data, these Gibbs energy functions were determined by including in the optimization procedure estimates of the entropy at high temperatures and the enthalpy of formation at 298.15 K. The estimation method has been described in recent articles [17,18,105–108]. Here we shall only summarize the main points. The theoretical background of some of the expressions used here can be found in, for example, a monograph by Grimvall [109].

### 5.1. General considerations

The temperature-dependent part of the function  ${}^0G_{\text{Zr,C}}(T)$  is usually dominated by the lattice vibrations, which may be described by a properly defined Debye temperature. Following Grimvall and Rosén [109,110] we use an entropy Debye temperature  $\Theta_S$ . It is obtained from the  $\Theta_S(T)$  function that reproduces the vibrational entropy  $S_{\text{vib}}(T)$  per mole of atoms of the compound if  $\Theta_S(T)$  is inserted in the expression for entropy  $S_D$  in the Debye model:

$$S_{\text{vib}}(T) = S_D[\Theta_S(T)/T] \quad (11)$$

At low temperatures ( $T \ll \Theta_S$ ),  $\Theta_S(T)$  varies with  $T$  because the true vibrational spectrum of the compound is not of the Debye form, and at high temperatures ( $T > \Theta_S$ ) it shows a smooth decrease with increasing  $T$ , caused by the anharmonic softening of the lattice vibrations. To obtain a stable value for  $\Theta_S$  we evaluate  $\Theta_S$  at  $T = \Theta_S$  and denote that  $\Theta_S$  by  $\Theta_S^0$ . The estimation procedure for high temperature entropy of metastable Zr carbides was based on constructing a probable  $\Theta_S(T)$  function. That was made in two steps. First the  $\Theta_S^0$  value was estimated and then we accounted for the decrease in  $\Theta_S$  with increasing  $T$  at  $T > \Theta_S$ . The estimation of  $\Theta_S^0$  relied on information about related systems, but  $\Theta_S^0$  is not directly suitable for such comparisons because it contains the contribution from the atomic masses. However, at high temperatures ( $T > \Theta_S/2$ ),  $\Theta_S$  essentially measures a logarithmic average of the phonon frequencies, and in that particular average the masses separate from the interatomic forces [109,110]. Therefore one can define a quantity  $k_S$ , with the dimension of a force constant (i.e. force per length), by

$$\Theta_S^0 = (\hbar/k_B)(k_S/M_{\text{eff}})^{1/2} \quad (12)$$

Here  $k_B$  and  $2\pi\hbar$  are Boltzmann's constant and Planck's constant respectively, and  $M_{\text{eff}}$  is the logarithmic average of the atomic masses. For a carbide  $\text{ZrC}_x$  we have

$$M_{\text{eff}}(\text{ZrC}_x) = (M_{\text{Zr}})^{1/(1+x)}(M_{\text{C}})^{x/(1+x)} \quad (13)$$

where  $M_{\text{Zr}}$  and  $M_{\text{C}}$  are the atomic masses of Zr and C.

The quantity  $k_S$ , which contains information on the strength of the average interatomic forces in the compound, has been [111] referred to as the "effective force constant". Previous studies based on  $k_S$  of the entropy of transition metals [111], and their combinations with C, N and B [110] revealed remarkable regularities, which have allowed the estimation of the  $k_S$  (and  $\Theta_S^0$ ) value for a substance from the  $k_S$  value of a related substance.

### 5.2. $k_S$ and $\Theta_S^0$ for Zr carbides

Recent studies of transition metal carbides [17,18], nitrides [17], and borides [112,113] have focused on the effect on  $k_S$  of changes in the average number  $n_e$  of valence electrons per atom. By applying interpolation and extrapolation procedures based on the assumption of a smooth variation of the cohesive properties with  $n_e$ , it has been possible to derive  $k_S$  (and  $\Theta_S^0$ ) values for various stable and metastable compounds. In Fig. 1 we plot, vs. the atomic fraction  $x_C$  of C in the compounds, the  $k_S$  value extracted from the entropy of h.c.p. Ti [111] and of TiC [18], and the  $k_S$  values for the metastable carbides  $\text{Ti}_3\text{C}_2$ ,  $\text{Ti}_2\text{C}$ ,  $\text{Ti}_7\text{C}_3$ ,  $\text{Ti}_5\text{C}_2$ ,  $\text{Ti}_3\text{C}$  and  $\text{Ti}_{23}\text{C}_6$  predicted in Ref. [18]. The information about Zr compounds is meagre, and we plot in Fig. 1 the  $k_S$  values for h.c.p. Zr [111], and the value  $k_S = 429 \text{ N m}^{-1}$  for ZrC (cF8), corresponding to  $\Theta_S^0 = 675 \text{ K}$ , which is obtained from the high temperature entropy arrived at in the present study. Lacking additional information, we estimated the  $k_S$  values of  $\text{ZrC}_{0.5}$  and  $\text{ZrC}_3$  by assuming that the variation in  $k_S$  with  $x_C$  for Zr carbides is similar to that shown by the results on Ti carbides. That variation is indicated in Fig. 1 using a broken line, which gave  $k_S = 337 \text{ N m}^{-1}$  for  $\text{ZrC}_{0.5}$  and  $k_S = 565 \text{ N m}^{-1}$  for  $\text{ZrC}_3$ . By combining these results with Eq. (12) we obtain the corresponding  $\Theta_S^0$  values, i.e. 505 K and 998 K respectively. All  $k_S$  and  $\Theta_S^0$  values relied on in this work are summarized in Table 1.

### 5.3. Temperature dependence of $\Theta_S$ and entropy functions for Zr carbides

According to the considerations of Section 5.1 the  $\Theta_S^0$  values estimated previously apply to a region of temperatures around  $T = \Theta_S^0$ . At higher temperatures

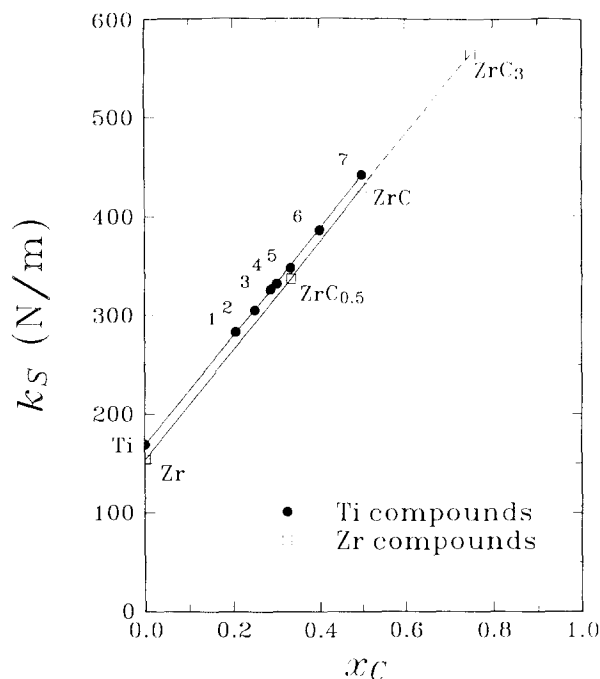


Fig. 1. The entropy related effective force constant  $k_S$  (Eq. (12)) for h.c.p. Ti [111], various Ti carbides [18], h.c.p. Zr [111] and the Zr carbides studied in the present work, as a function of the atomic fraction  $x_C$  of carbon in the compound. The numbers refer to (1)  $Ti_{23}C_6$ , (2)  $Ti_3C$ , (3)  $Ti_5C_2$ , (4)  $Ti_7C_3$ , (5)  $Ti_2C$ , (6)  $Ti_3C_2$  and (7)  $TiC$ .

$\Theta_S(T)$  is expected to decrease because of anharmonic effects, but a method for predicting the magnitude of the effect has not yet been developed. In the studies reported in Refs. [105] and [106] such an effect for a compound was estimated by comparing with the  $\Theta_S(T)$  vs.  $T$  functions of compounds in the same system. Lacking information about Zr carbides we estimated the temperature dependence of their  $\Theta_S(T)$  function by applying a scaling relation, previously used in a study of the W–N system [115], which makes use of information on  $\Theta_S(T)$  for ZrC. Values of  $\Theta_S$  for  $ZrC_{0.5}$  and  $ZrC_3$  at various  $T$  were derived by combining their  $\Theta_S^0$  values with an estimate of their  $\Theta_S(T)/\Theta_S^0$  vs.  $T/\Theta_S^0$  function based on assuming that this function is the same as

evaluated for ZrC (cF8) from the entropy values obtained in the present assessment, and neglecting electronic contributions.

The  $\Theta_S(T)$  functions, arrived at here, were used to calculate  $S_{vib}(T)$  values from Eq. (11) at various temperatures. Then we neglected non-vibrational contributions and treated those values as approximations of the total entropy of Zr carbides and used them in evaluating the temperature dependent part of  $\Delta^0G^\phi(T)$  ( $\phi = \alpha, \beta$ ) (Eq. (6)). The coefficients  $b^\phi$ ,  $c^\phi$ ,  $d^\phi$ ,  $e^\phi$ ,  $f^\phi$  and  $g^\phi$  obtained in this way were not allowed to change during the optimization of the experimental data selected in Section 4.

#### 5.4. Enthalpy of formation of metastable Zr carbides

Another useful finding of recent work on the cohesive properties of 3d transition metal carbides and nitrides [17,18] is that the enthalpy  $\Delta^0H_a(298.15)$  of formation at 298.15 K, expressed per mole of atoms in the compound varies smoothly with  $n_c$ . By using this fact it has been possible to derive new  $\Delta^0H_a(298.15)$  values for various stable and metastable carbides [18] and nitrides [17,116] of Sc, Ti, V, Cr, Mn, Fe, Co and Ni. Since the complex, metastable carbides of metals from the 4d transition series have not yet been studied, we tentatively estimated the enthalpy of formation of  $ZrC_{0.5}$  and  $ZrC_3$  by combining the  $\Delta^0H_a(298.15)$  value for ZrC (cF8) with the assumption that the  $\Delta^0H_a(298.15)$  vs.  $x_C$  function for Zr carbides is similar to that obtained for Ti carbides in Ref. [18]. Lacking direct measurements these estimates were treated as true experimental values and included in the optimization of the Zr–C system, together with the information selected in Section 4. By searching for the best fit to the set of input data it was possible to determine the  $a^\phi$  coefficients of the polynomial in Eq. (6). The  $\Delta^0H_a(298.15)$  values obtained in this work (Table 1) will be compared in Section 6 with the predictions of the semiempirical scheme developed by Miedema and coworkers [114].

Table 1  
Properties of various stable and metastable Zr carbides

Compound	Structure (Pearson symbol)	$n_c$ (e atom <sup>-1</sup> )	$k_S$ (N m <sup>-1</sup> )	$\Theta_S^0$ (K)	$-\Delta^0H_a$ (kJ (mol atoms) <sup>-1</sup> )	
					Present study	Previous work
$ZrC_{0.5}$	(hP3)	4.0	337	505	103.5	103* (see Table 7)
ZrC	(cF8)	4.0	429	675	69	71*
$ZrC_3$	Based on b.c.c. Zr	4.0	565	998	25 ( $\pm 25$ )	53*

\*Predicted by the Miedema approach [114].

## 6. Results and discussion

A summary of the optimum parameters describing the thermodynamic properties of the Zr–C system is presented in Table 2. In the present section this thermodynamic description is used to calculate the Zr–C phase diagram and other properties. Comparisons with the available information are made in a series of graphics and tables, and even involve data which were not included in the optimization procedure. All thermodynamic calculations reported in the following were performed by using the THERMO-CALC [117,118] program.

### 6.1. The phase diagram

The Zr–C phase diagram, calculated by using the thermodynamic description in Table 2, is presented in Fig. 2 and compared in Fig. 3 with experimental information. Among the experimental data shown in these graphics there are those which concern the melting temperatures of the  $ZrC_x$  phase. The metallographic observations by Sara [59] and most of the results by Zotov and Kotelnikov [63] shown in Fig. 3(a) and by Rudy [62] in Fig. 3(b) are reasonably well accounted for by the calculation. In Fig. 3(a) there is a data point due to Zotov and Kotelnikov [63] which falls above the liquidus line, whereas the points from the remaining alloys studied by them are consistent with the present calculation. It seems quite possible that the solidus temperature determined from this alloy by Zotov and Kotelnikov [63] is too high.

The temperature and composition of the congruent melting point of  $ZrC_x$  are compared in Table 3 with values according to various authors [24,25,27,53–63,120].

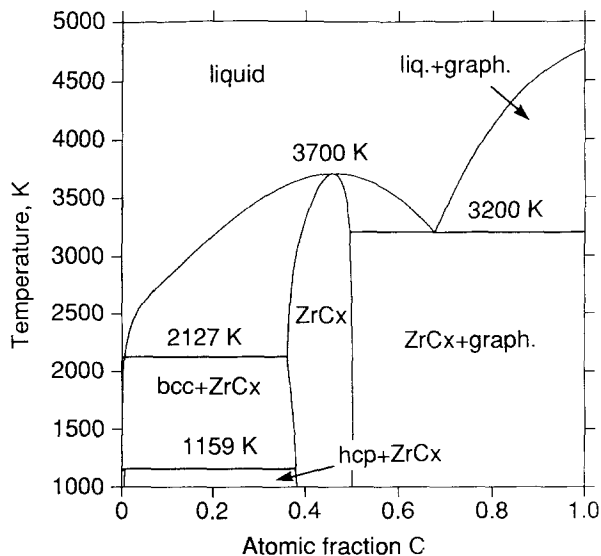


Fig. 2. The Zr–C phase diagram (—) calculated using the present thermodynamic description.

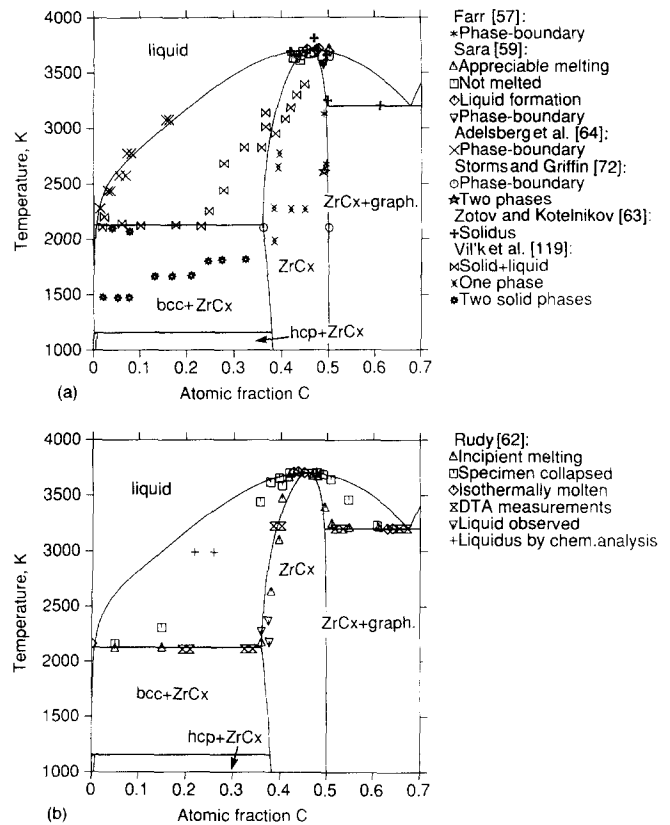


Fig. 3. (a) The Zr–C phase diagram (—) calculated using the present thermodynamic description, compared with experimental data (symbols). (b) The Zr–C phase diagram (—) calculated using the present thermodynamic description, compared with experimental data (symbols).

The present values agree, within the experimental uncertainty, with the results by Sara [59] and Rudy and coworkers [60–62], and with the recommendations of Storms [24], Shunk [25] and Kubaschewski-von Goldbeck [27]. Contrasting with this, the Zr–C phase diagram included in the most recent compilation of binary systems [2], which is due to Okamoto [28], is based on a temperature and composition for the congruent melting of  $ZrC_x$  that are almost identical to the result by Zotov and Kotelnikov [63] referred to above.

Fig. 3 shows some data points [60,63] concerning the temperature of the  $\gamma + \text{liquid} + \text{graphite}$  equilibrium. In Table 4 a detailed comparison is given with previously reported values for the temperature, and the composition of the various phases taking part in this equilibrium. The present value for the  $\gamma + \text{liquid} + \text{graphite}$  equilibrium temperature reproduces the result by Zotov and Kotelnikov [63] and is almost identical to that measured by Portnoi et al. [67]. In addition, it falls within the experimental uncertainty of the values reported by Rudy et al. [60], Adelsberg et al. [69], Rudy and Progulski [61] and Rudy [62]. The remaining measurements of the three-phase equilibrium temperature, and the values preferred by Storms [24], Shunk [25] and Kubaschewski-von Goldbeck [27], are lower than

Table 2

Summary of the optimum parameters describing the thermodynamic properties of the Zr–C system

B.c.c. ( $\beta$ ) phase with formula  $(Zr)_1(C, Va)_3$ 298.15 K <  $T$  < 2128 K

$${}^0G_{Zr,Va}^{\beta} - H_{Zr}^{SER} = -525.539 + 124.9457T - 25.607406T \ln T \\ - 3.40084 \times 10^{-4}T^2 - 9.729 \times 10^{-9}T^3 + 25.233T^{-1} \\ - 7.6143 \times 10^{-11}T^4$$

2128 K <  $T$  < 6000 K

$${}^0G_{Zr,Va}^{\beta} - H_{Zr}^{SER} = -30\,705.955 + 264.284163T - 42.144T \ln T \\ + 1.276058 \times 10^{32}T^{-9}$$

$$* {}^0G_{Zr,C}^{\beta} - H_C^{SER} - 3H_{Zr}^{SER} = -142\,838.2 + 631.7121T - 96.28173T \ln T \\ - 1.856037 \times 10^{-3}T^2 - 9.296\,8513 \times 10^{-8}T^3 + 2\,261356T^{-1} \\ - 7.933899 \times 10^9T^{-3}$$

$$* {}^0L_{Zr,C,Va}^{\beta} = -223\,221.3$$

F.c.c. ( $\gamma$ ) phase with formula  $(Zr)_1(C, Va)_1$ 

$${}^0G_{Zr,Va}^{\gamma} - H_{Zr}^{SER} = 7600 - 0.9T + GZRHCP$$

$$* {}^0G_{Zr,C}^{\gamma} - H_C^{SER} - H_{Zr}^{SER} = -224\,784.9 + 297.0288T - 48.14055T \ln T \\ - 1.372273 \times 10^{-3}T^2 - 1.015994 \times 10^{-7}T^3 \\ + 517\,213.0T^{-1} - 8.300\,54316 \times 10^8T^{-3}$$

$$* {}^0L_{Zr,C,Va}^{\gamma} = -41\,870.20 - 35.70271T + 6.042424T \ln T \\ - 1.326472 \times 10^{-3}T^2$$

$$* {}^1L_{Zr,C,Va}^{\gamma} = -81\,870.20 - 35.70271T + 6.042424T \ln T \\ - 1.326472 \times 10^{-3}T^2$$

H.c.p. ( $\alpha$ ) phase with formula  $(Zr)_1(C, Va)_{0.5}$ 298.15 K <  $T$  < 2128 K

$${}^0G_{Zr,Va}^{\alpha} - H_{Zr}^{SER} = GZRHCP$$

2128 K <  $T$  < 6000 K

$${}^0G_{Zr,Va}^{\alpha} - H_{Zr}^{SER} = -26\,085.921 + 262.724183T - 42.144T \ln T \\ - 1.342895 \times 10^{31}T^{-9}$$

$$* {}^0G_{Zr,C}^{\alpha} - 0.5H_C^{SER} - H_{Zr}^{SER} = -115\,822.7 + 212.2971T - 36.10565T \ln T \\ - 1.375489 \times 10^{-3}T^2 - 1.361587 \times 10^{-7}T^3 + 217\,131.0T^{-1} - 1.9505689 \times 10^8T^{-3}$$

$$* {}^0L_{Zr,C,Va}^{\alpha} = 3206.881$$

Liquid (liq) phase with formula  $(Zr, C)$ 

$${}^0G_C^{liq} - H_C^{SER} = 117\,369 - 24.63T + GCLIQ$$

298.15 K <  $T$  < 2128 K

$${}^0G_{Zr}^{liq} - H_{Zr}^{SER} = 18\,147.69 - 9.080812T + 1.6275 \times 10^{-22}T^7 + GZRHCP$$

2128 K <  $T$  < 6000 K

$${}^0G_{Zr}^{liq} - H_{Zr}^{SER} = 17\,804.661 - 8.911574T + 1.342895 \times 10^{31}T^{-9} + GZRLIQ$$

$$* {}^0L_{Zr,C}^{liq} = -305\,420.6 + 16.01676T$$

$$* {}^1L_{Zr,C}^{liq} = -39\,269.66$$

$$* {}^2L_{Zr,C}^{liq} = 50\,000$$

Symbols

$$GCLIQ = -17\,368.441 + 170.73T - 24.3T \ln T - 4.723 \times 10^{-4}T^2 \\ + 2\,562600T^{-1} - 2.643 \times 10^8T^{-2} + 1.2 \times 10^{10}T^{-3}$$

$$GZRHCP = -7829 + 125.649T - 24.1618T \ln T - 0.00437791T^2 \\ + 34\,971T^{-1}$$

$$GZRLIQ = -26\,085.921 + 262.724183T - 42.144T \ln T \\ - 1.342895 \times 10^{31}T^{-9}$$

Values are given in SI units and correspond to one mole of formula units. The parameters marked with an asterisk (\*) were assessed in the present work.

Table 3

The temperature and composition for the congruent melting of the  $ZrC_x$  ( $\gamma$ ) phase (the temperature values reported by the various authors have been corrected by us to the IPTS68 temperature scale)

Reference	Year	$T$ (K) (IPTS68)	$x_{C^\gamma}$	Comments
Friederich and Sitting [53]	1925	3400–3500	–	Estimated in Ref. [53] from experiments
Agte and Alterthum [54]	1930	$3784 \pm 125$	–	Pyrometry, metallographic observations
Glaser [55]	1953	$3455 \pm 50$	–	Unpublished work
Brownlee [56]	1958	3816	–	Disappearing filament optical pyrometry
Farr [57]	1962	$3700 \pm 50$	$0.45 \pm 0.06$	Unpublished work
Paderno [58]	1962	4016	–	Experimental value
Wilhelm et al. [120]	1964	3530	–	Experimental value
Sara [59]	1965	3700	0.46	Annealing, optical pyrometry, macroscopic and metallographic examination of the samples
Rudy et al. [60]	1965	$3720 \pm 20$	0.45	Annealing, optical pyrometry, macroscopic and metallographic examination of the samples
Storms [24]	1967	$3700 \pm 20$	0.45	Selected values
Rudy and Progulski [61]	1967	$3720 \pm 25$	$0.45 \pm 0.01$	Resistance heating, and optical pyrometry using a disappearing filament type micropyrometer
Rudy [62]	1969	$3725 \pm 25$	$0.44 \pm 0.01$	Determination of incipient melting and isothermal melting of alloys
Shunk [25]	1969	3700	0.46	Selected values
Zotov and Kotelnikov [63]	1975	$3810 \pm 70$	0.465	Optical pyrometry and metallographic examination of the samples
Kubaschewski-von Goldbeck [27]	1976	$\approx 3700$	0.46	Selected values
Okamoto [28]	1990	3813	0.465	Selected values
Present work		3700	0.458	Assessment based on thermodynamic calculations

the present temperature. However, our result agrees with the value chosen by Okamoto [28] in the most recent review of the Zr–C phase diagram. The calculated value for the composition of the  $ZrC_x$  ( $\gamma$ ) phase at the three-phase equilibrium agrees well with the available information, but the calculated carbon content  $x_C = 0.676$  of the liquid phase is larger than those found in the literature, which vary between 0.644 and 0.655 (Table 4). We remark that the agreement between the calculation and this experimental value could not be improved by us, while keeping a good agreement with Adelsberg et al.'s [64] data on the position of the liquid–liquid +  $\gamma$  equilibrium boundary on the Zr-rich side of the phase diagram. The reason for this discrepancy was not found, and we only summarize the possible explanations: (i) the reported carbon content at the  $\gamma$  + liquid + graphite equilibrium is about 2 at.% too low, (ii) that carbon content is correct, but the solubility of  $\gamma$  in the Zr-rich liquid phase according to Adelsberg et al. [64] is too low, i.e. the liquid +  $\gamma$  two-phase field is not as wide as in Fig. 3, and (iii) both

the eutectic composition and the data by Adelsberg et al. [64] are correct, but the substitutional, Redlich–Kister [49] description of the liquid phase is less accurate at high carbon contents and in the presence of strong metal–carbon interactions. Additional experimental data would help to test possibilities (i) and (ii), whereas the applicability of the Redlich–Kister model could be tested by analysing other Me–C systems involving strong carbide formers of the transition series, e.g. the Ta–C or the Hf–C systems. This problem will be dealt with in future work.

The calculated equilibrium boundaries of the  $ZrC_x$  ( $\gamma$ ) phase in Fig. 3 account for the experimental results by Farr [57], Sara [59], Rudy [62], Storms and Griffin [72] and by Zotov and Kotelnikov [63]. Fig. 3(a) also shows the constitution of the experimental alloys studied by Vil'k et al. [119]. They are in agreement with the present boundaries for the  $\gamma$  phase, except for those with more than about 40 at.% C, where they found a two-phase state of  $\gamma$  + liquid. The present study suggests that these results are probably in error.

Table 4

The temperature and composition of the  $ZrC_x$  ( $\gamma$ ) phase and the liquid phase at the  $\gamma$ +liquid+graphite three-phase equilibrium

Reference	Year	T (K) (IPTS68)	$x_C^{\gamma\text{-liq+graph}}$	$x_C^{\text{liq-}\gamma\text{+graph}}$	Comments
Agte and Moers [65]	1931	2697	–	–	Experimental value
Chiotti and Weiner [66]	1950	3078 ± 50	–	0.644	Experimental value
Portnoi et al. [67]	1961	3199 ± 50	–	–	Experimental value
Farr [57]	1962	3128 ± 50	0.491	–	Unpublished work
Wallace et al. [68]	1963	3148 ± 30	–	–	Optical pyrometry and a thermal arrest apparatus
Kendall et al. [121]	1965	–	–	0.655	Experimental value
Sara [59]	1965	3128	0.491	0.65	Optical pyrometry, DTA, macroscopic and metallographic examination of the samples; the composition of the $ZrC_x$ ( $\gamma$ ) phase was taken from Farr [57]
Rudy et al. [60]	1965	3190 ± 12	(≤0.5)	0.645 ± 0.005	Optical pyrometry, DTA, macroscopic and metallographic examination of the samples
Adelsberg et al. [69]	1966	3168 ± 50	–	–	Thermal analysis on heating and cooling; isothermal annealing followed by macroscopic and metallographic examination of the samples; use of an optical pyrometer and two-colour pyrometers
Rudy and Progulski [61]	1967	3190 ± 19	–	0.645 ± 0.01	Optical pyrometer using a disappearing filament type micropyrometer
Storms [24]	1967	3128 ± 50	0.492	0.64 ± 0.66	Selected values
Nickel et al. [122]	1968	–	0.50	–	Metallographic and X-ray examination of the samples; electron microprobe analysis
Rudy [62]	1969	3189 ± 18	0.494	0.645 ± 0.01	DTA and observation of the incipient melting and isothermal melting of alloys; the composition of the $ZrC_x$ ( $\gamma$ ) phase was taken from Farr [57]
Shunk [25]	1969	3128 ± 50	0.491	0.65	Selected values
Zotov and Kotelnikov [63]	1975	3200 ± 50	–	–	Optical pyrometry and metallographic observation of the samples
Kubaschewski-von Goldbeck [27]	1976	3128	(≈0.49)	≈0.65	Selected values
Okamoto [28]	1990	3200	0.496	≈0.65	Selected values
Present work		3200	0.495	0.676	Assessment based on thermodynamic calculations

The temperature values reported by the various authors have been corrected by us to the IPTS68 temperature scale. Compositions given in parentheses refer to values estimated in the original works, or taken by us from the phase diagrams drawn by the various authors.

The calculated liquid–liquid +  $\gamma$  equilibrium boundary at the Zr-rich side of the phase diagram in Fig. 3(a) reproduces the solubility data by Adelsberg et al. [64] and is compatible with the constitution of the experimental alloys studied by Vil'k et al. [119]. Among the results by Rudy [62] in Fig. 3(b), there are two points concerning the position of the liquid–liquid +  $\gamma$  equilibrium boundary which indicate a larger solubility of  $ZrC_x$  ( $\gamma$ ) in the liquid than according to Adelsberg et al. [64] and thus fall to the right of the calculated line.

In Fig. 3 there are data points concerning the  $\beta$ +liquid +  $\gamma$  three-phase equilibrium temperature. In Table 5 a detailed comparison is given with previously reported values for the temperature and composition of the  $\beta$ , liquid and  $\gamma$  phases at the three-phase equilibrium. The present value for the three-phase equilibrium temperature reproduces exactly the result by Bhatt et al. [71]. In addition, it falls between the values from Sara [59] and Rudy and coworkers [60–62]. The temperature values recommended by Shunk [25] and Kubaschewski-

Table 5  
The temperature and composition of the  $\beta$ , liquid and  $ZrC_x$  ( $\gamma$ ) phase at the  $\beta$ +liquid+ $\gamma$  three-phase equilibrium

Reference	Year	T (K) (IPTS68)	$x_C^{\beta\text{-liq}+\gamma}$	$x_C^{\text{liq}-\beta+\gamma}$	$x_C^{\gamma-\beta+\text{liq}}$	Comments
Hayes [21]	1955	2126	$\approx 0$	$\approx 0$	0.5	Selected values
Benesovsky and Rudy [70]	1960	2106	( $\approx 0.01$ )	$< 0.05$	$0.30 < x_C < 0.35$	Metallographic and X-ray examination; a tentative phase diagram is presented
Farr [57]	1962	2086	–	–	0.355	Unpublished work
Sara [59]	1965	2136	(Negligible)	$\approx 0.01$	0.385	DTA measurements on heating and cooling; annealing, macroscopic and metallographic examination
Rudy et al. [60]	1965	$2111 \pm 5$	(Negligible)	$< 0.05$	0.375	DTA measurements; annealing, macroscopic and metallographic examination
Rudy and Progulski [61]	1967	$2111 \pm 20$	–	$0.03 \pm 0.015$	–	Optical pyrometry using a disappearing filament type pyrometer
Storms [24]	1967	$2111 > T > 2086$	(Negligible)	(Negligible)	$0.355 < x_C < 0.375$	Selected values
Nickel et al. [122]	1968	–	–	–	0.384	Metallographic and X-ray examination of the samples; electron microprobe analysis
Rudy [62]	1969	$2111 \pm 20$	( $< 0.01$ )	$0.03 \pm 0.015$	$0.375 \pm 0.005$	DTA and observation of the incipient melting and isothermal melting of alloys; annealings and quenching; metallographic examination
Shunk [25]	1969	2136	(Negligible)	$\approx 0.01$	0.385	Selected values
Storms and Griffin [72]	1973	(2103)	–	–	0.361	Equilibrium boundary for $ZrC_x$ at 2103 K; from Zr activity data obtained by mass spectrometry
Kubaschewski-von Goldbeck [27]	1976	2136	(Negligible)	$\approx 0.01$	0.375	Selected values
Bhatt et al. [71]	1987	$2127 \pm 5$	–	–	–	Use of the “spot technique”, involving heating of the sample in an effusion cell; optical pyrometry using a disappearing filament type optical pyrometer
Okamoto [28]	1990	2078	( $\approx 0.01$ )	( $\approx 0.02$ )	$\approx 0.33$	Selected values
Present work		2127	0.005	0.006	0.359	Assessment based on thermodynamic calculations

The temperature values reported by the various authors have been corrected by us to the IPTS68 temperature scale. Values given in parentheses refer to those estimated in the original works, or taken by us from the phase diagrams drawn by the various authors.

von Goldbeck [27] are only 9 K higher than the present temperature, but the value selected by Okamoto [28] is lower than the present and the remaining values in Table 5. The present value for the composition of the  $\gamma$  phase in equilibrium with  $\beta$  and liquid agrees well with the results by Farr [57] and Storms and Griffin [72]. The compositions of the  $\beta$  and liquid phases are not known with accuracy and our calculated values are in line with the low carbon solubilities expected or estimated in previous reviews of the Zr–C phase diagram.

Finally, Table 6 demonstrates that the present calculation of the  $\alpha+\beta+\gamma$  three-phase equilibrium tem-

perature reproduces exactly the differential thermal analysis (DTA) result by Sara [59]. The calculated compositions of the  $\alpha$ ,  $\beta$  and  $\gamma$  phases are in line with the estimated values that have been recommended in previous work.

## 6.2. Thermochemical properties

### 6.2.1. Stable phases

The calculated enthalpy of formation of the  $ZrC_x$  phase as a function of composition (full line) is compared in Fig. 4 with experimental results from various authors (symbols). The calculated line accounts well for the data by Baker et al. [79]. A comparison concerning

Table 6

The temperature and composition of the  $\alpha$ ,  $\beta$  and  $\text{ZrC}_x$  ( $\gamma$ ) phase at the  $\alpha+\beta+\gamma$  three-phase equilibrium

Reference	Year	T (K) (IPTS68)	$x_{\text{C}}^{\alpha-\beta+\gamma}$	$x_{\text{C}}^{\beta-\alpha+\gamma}$	$x_{\text{C}}^{\gamma-\alpha+\beta}$	Comments
Hayes [21]	1955	1139	(Negligible)	(Negligible)	(0.5)	Recommended phase diagram
Benesovsky and Rudy [70]	1960	(1173)	(<0.01)	( $\approx 0.02$ )	( $\approx 0.36$ )	Estimated values
Sara [59]	1965	1159	–	–	–	DTA
Rudy et al. [60]	1965	$1146 \pm 15$	(Negligible)	(Negligible)	(0.375)	DTA
Storms [24]	1967	$1146 \leq T \leq 1159$	(<0.01)	( $\approx 0.015$ )	(0.375)	
Shunk [25]	1969	(1139)	(Negligible)	(Negligible)	(0.40)	Recommended phase diagram
Kubaschewski-von Goldbeck [27]	1976	(1146)	(Negligible)	(Negligible)	0.40	
Okamoto [28]	1990	(1136)	(Negligible)	(Negligible)	( $\approx 0.38$ )	
Present work		1159	0.0073	$1.4 \times 10^{-5}$	0.379	Assessment based on thermodynamic calculations

The temperature values reported by the various authors have been corrected by us to the IPTS68 temperature scale. Values given in parentheses refer to those estimated in the original works, or taken by us from the phase diagrams drawn by the various authors.

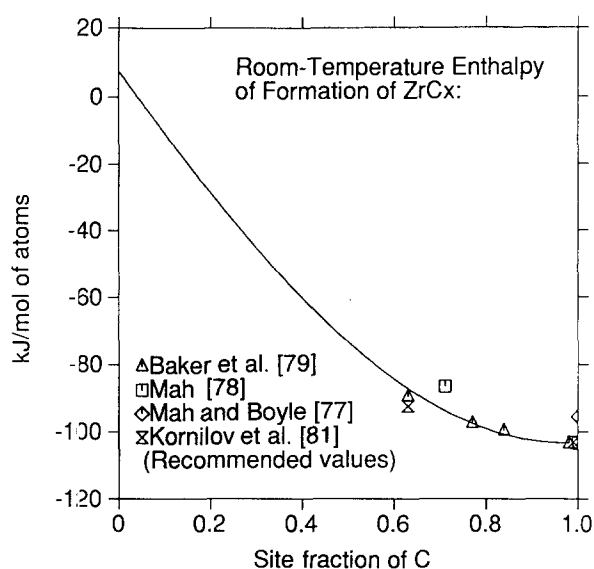


Fig. 4. The calculated enthalpy of formation per mole of atoms of the  $\text{ZrC}_x$  carbide at 298.15 K (—) as a function of the fraction of C atoms in its sublattice, compared with experimental data (symbols).

the enthalpy of formation of the stoichiometric  $\text{ZrC}$  carbide is given in Table 7. The present result agrees with the values recommended in recent work [19,80] but is more negative than those selected by Schick [30] and Hultgren et al. [26]. In particular, our value is more negative than that obtained in the JANAF tables [32] by averaging vaporization data by Pollock [83] and Vidale [123] with the combustion calorimetry result by Mah [78].

The thermal properties of the  $\text{ZrC}_x$  ( $\gamma$ ) phase at high temperatures were determined from measurements of the so-called heat content, i.e. of  ${}^0H_m^{(\gamma)}(T) - {}^0H_m^{(\gamma)}(T_0)$ , where  $T_0$  is a reference temperature. When selecting experimental values for the optimization procedure, and in comparing enthalpy calculations with experiments, it has been useful to consider the quantity usually called mean heat capacity, which is obtained from values of the heat content as follows:

mean heat capacity

$$= [{}^0H_m^{(\gamma)}(T) - {}^0H_m^{(\gamma)}(T_0)] / (T - T_0) \quad (14)$$

The use of this quantity is illustrated in Figs. 5 and 6. In Fig. 5 we compare the calculated heat content of the  $\text{ZrC}_x$  phase with experiments by Neel et al. [86], Mezaki et al. [88], and Levinson [89]. This graphic gives the impression that the calculated line falls in the scatter band of the measured values. However, a comparison with the same data expressed as mean heat capacity values, which is given in Fig. 6, demonstrates that the values by Neel et al. [86] are too scattered to be used in the evaluation and also that there is a systematic deviation between the present description and the data by Levinson [89] and Mezaki et al. [88]. As a consequence, the enthalpy values arrived at by Storms and Griffin [72] by combining experiments from those two [88,89] sources are also larger than the calculated values. A comparison between the present description and the mean heat capacity values by Bolgar

Table 7

The enthalpy of formation of the stoichiometric ZrC( $\gamma$ ) phase, at 298.15 K and 101 325 Pa according to various authors

Reference	Year	$-\Delta^{\circ}H_{\text{f}}(298.15)$ (kJ (mol atoms) <sup>-1</sup> )	Comments
Mah and Boyle [77]	1955	92.3 ± 3	From combustion calorimetry data; based on the heat of formation of ZrO <sub>2</sub> reported by Humphrey [75]
Pollock [83]	1961	99.8 ± 10	From studies of the vaporization behaviour of ZrC <sub>x</sub> using the Knudsen and Langmuir techniques
Coffman et al. [84]	1963	99.4	From studies of the vaporization behaviour of ZrC <sub>x</sub> using the Langmuir method; value quoted by Hultgren et al. [26]
Mah [78]	1964	97.5 ± 3	From combustion calorimetry data; based on the heat of formation of ZrO <sub>2</sub> reported by Humphrey [75]
Schick [30]	1966	100	Selected value
Baker et al. [79]	1969	103.6 ± 1.3	Extrapolation to stoichiometry of combustion calorimetry data; based on the heat of formation of ZrO <sub>2</sub> reported by Huber et al. [76]
Hultgren et al. [26]	1973	98.3	Selected value
Kornilov et al. [81]	1975	103.3 ± 3	Extrapolation to stoichiometry of an expression based on their own [81] and Baker et al.'s [79] calorimetric data
Alcock et al. [31]	1976	103.0 ± 1.3	Selected value for ZrC <sub>0.96</sub> , based on the results by Baker et al. [79]
Maslov et al. [82]	1978	99.2 ± 2	Estimated from their own combustion calorimetry data
Kubaschewski and Alcock [80]	1983	103.0 ± 1.3	Selected value
Chase et al. [32] (JANAF)	1985	98.3 ± 6.5	Selected value; corresponds to an evaluation from 1964; it is based on results by Pollock [83], Vidale [123] and Mah [78]
Fernández Guillermet et al. [19]	1992	103.6 ± 3	Selected value
Present work		103.5	Assessment based on thermodynamic calculations

et al. [90] and Kantor and Fomichev [91] is given in Fig. 7, and in Fig. 8 we compare calculations with the experimental results by Turchanin and Fesenko [92]. The results from these various sources, which were included in the present optimization, are reproduced by the assessed description of the ZrC<sub>x</sub> phase. In addition, the present values for ZrC agree with those obtained by Sheindlin et al. [98] by extrapolating to stoichiometry enthalpy data for two samples with different amounts of excess carbon. This is shown in Fig. 9. Finally, in Fig. 10 we compare our calculated mean heat capacity values for ZrC with the values recommended by Schick [30] and Hultgren et al. [26] and in the JANAF tables [32]. The present study leads to smaller heat content values for ZrC than those obtained in previous assessments, except for the values proposed by Hultgren et al. [26] for the high temperature range.

The present assessment of the ZrC<sub>x</sub> ( $\gamma$ ) phase used heat capacity information only for the low temperature range, i.e. the measurements performed by Westrum and Feick [85] between 5 and 350 K. Fig. 11 demonstrates that their values for temperatures higher than 150 K

are well reproduced by the calculation. In Fig. 12 we compare our calculations with measurements of  $C_p$  which were not used in the present evaluation. The calculated line falls in the scatter band of the measured values and agrees better with the results by Valentine et al. [99] at low temperatures and with the results by Petrova and Chekhovskoi [103] for temperatures around 2000 K. Some of the results by Mebed et al. [101] from temperatures around 2000 K are also close to the calculated line but, in general, their values suggest a more rapid increase in  $C_p$  with temperature than that obtained by us. The data by Kolesnichenko and Pustogarov [102] for temperatures above 2000 K deviate systematically from the present values but show a similar variation in  $C_p$  with  $T$ , whereas the results from McDonald et al. [100], which fall below the calculated line, are too scattered to be used in determining a temperature effect on  $C_p$ . A comparison between the present  $C_p$  vs.  $T$  function and that suggested by Storms and Griffin [72] was given in Fig. 11. In Fig. 13 we extend the comparison to the  $C_p$  values recommended by Schick [30], Hultgren et al. [26], and the JANAF

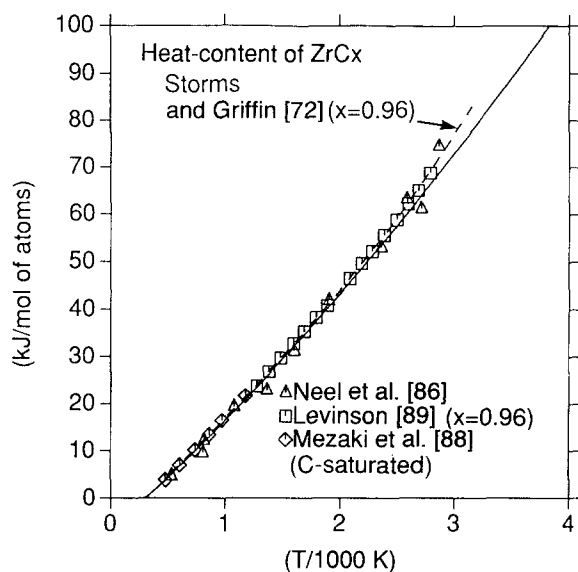


Fig. 5. The calculated heat content of the  $ZrC_{0.96}$  carbide as a function of temperature (—) compared with experimental data (symbols) and the values recommended by Storms and Griffin [72] (---).

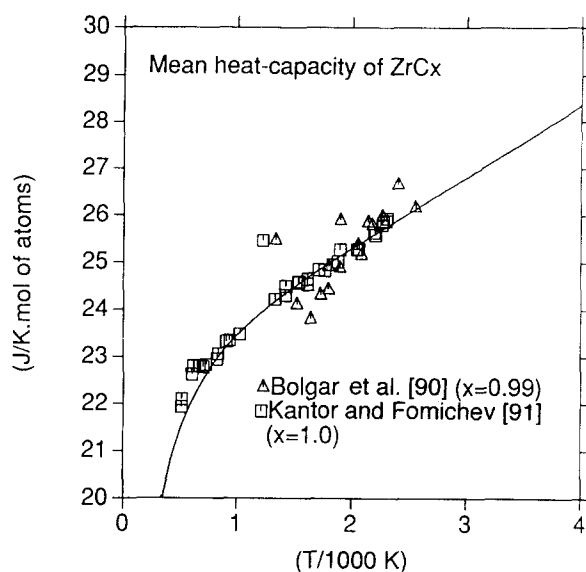


Fig. 7. The calculated mean heat capacity (Eq. (14)) of the  $ZrC_x$  carbide as a function of temperature (—) compared with experimental data (symbols).

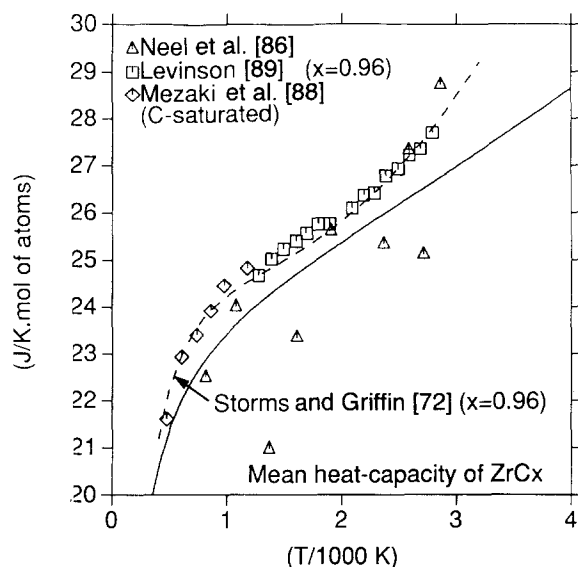


Fig. 6. The calculated mean heat capacity (Eq. (14)) of  $ZrC_{0.96}$  as a function of temperature (—) compared with experimental data (symbols) and the values recommended by Storms and Griffin [72] (---).

tables [32]. Finally, in Fig. 14 we show the entropy vs. temperature functions for  $ZrC$  proposed in previous analyses [26,30,32] together with our results. The present assessment leads to smaller entropy values at high temperatures than those given in compilations by Schick [30] and Hultgren et al. [26] and in the JANAF tables [32].

Additional information on the thermochemical properties of the  $ZrC_x$  ( $\gamma$ ) phase at high temperatures was extracted in this study from measurements of the Zr activity by Storms and Griffin [72], and Andrievskii et

al. [104]. In Figs. 15 and 16 we compare the calculated composition dependence of the Zr activity in the  $ZrC_x$  ( $\gamma$ ) phase at 2103 K and 2500 K, referred to liquid Zr, with experimental data from Storms and Griffin [72] and Andrievskii et al. [104] respectively. The calculated line falls in the experimental scatter band. Fig. 17 gives a comparison between calculated and measured Zr activities at the  $ZrC_x$  + graphite two-phase equilibrium at 1 atm, referred to liquid Zr, as a function of temperature. The present values account well for the measurements by Storms and Griffin [72].

We close this section on the thermochemical properties of the stable phases in the Zr–C system by considering the Gibbs energy of formation of the C-saturated  $ZrC_x$  ( $\gamma$ ) phase. A calculation based on the present description, using liquid phase as a reference state for pure Zr, and expressing the results in joules per mole of  $ZrC_x$ , is compared in Fig. 18 with results from previous work. The calculated line passes through the values obtained by Storms and Griffin [72] from their experiments in Fig. 17, but there are six data points from the lowest part of the temperature range studied by them which deviate negatively from our results. The existence of this discrepancy can be understood by referring to Fig. 17, which shows that those points from the lowest temperature fall, indeed, below the calculated line. Storms and Griffin [72] made a comparison like that in Fig. 18 using their own thermal functions for  $ZrC_{0.96}$  and found a large discrepancy between experimental and assessed Gibbs energies of formation. In particular, they noted that the experimental data points seem to indicate a different slope for the Gibbs energy of formation vs. temperature function and concluded that the thermal functions of

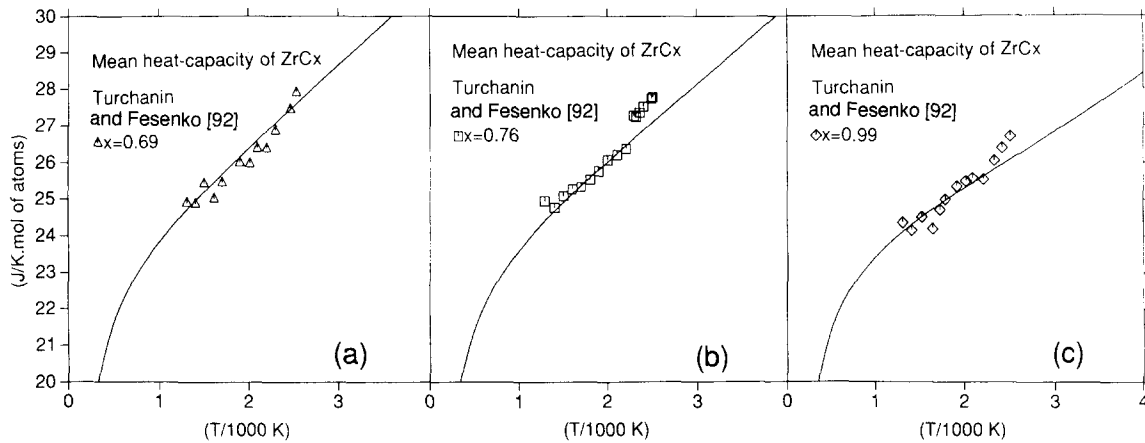


Fig. 8. The calculated mean heat capacity (Eq. (14)) of  $ZrC_x$  carbides with (a)  $x=0.69$ , (b)  $x=0.76$  and (c)  $x=0.99$ , as a function of temperature compared with experimental data (symbols).

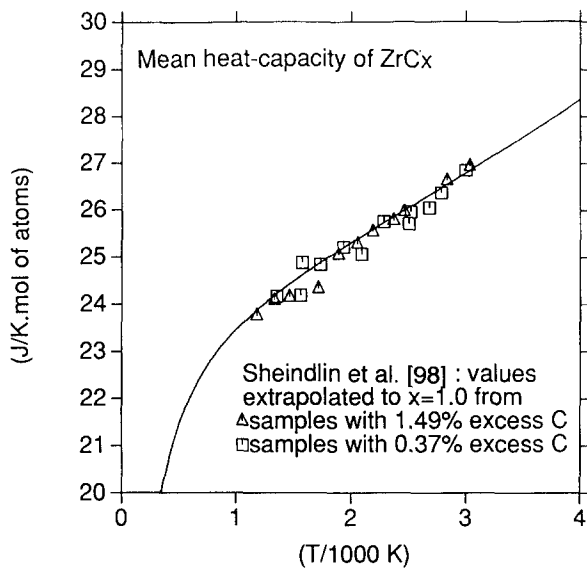


Fig. 9. The calculated mean heat capacity (Eq. (14)) of the ZrC carbide as a function of temperature (—) compared with values obtained by Sheindlin et al. [98] (symbols).

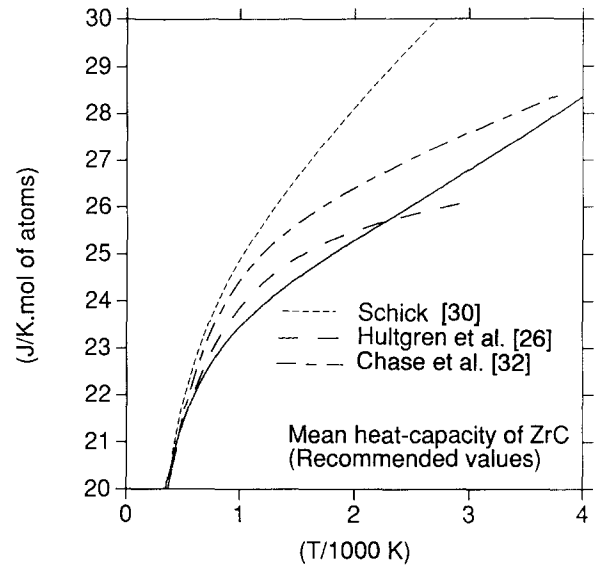


Fig. 10. The calculated mean heat capacity (Eq. (14)) of the ZrC carbide as a function of temperature (—) compared with the values recommended by Schick [30] and Hultgren et al. [26] and in the JANAF thermochemical tables [32].

liquid Zr, which they took from Hultgren et al. [26], were probably erroneous. Contrasting with that, the present analysis, which is based on a more recent description of liquid Zr [39] and various kinds of information about the thermodynamics of the  $ZrC_x$  ( $\gamma$ ) phase, leads to good agreement with the Gibbs energy values from Storms and Griffin [72] (Fig. 18). In addition, the Gibbs energy of formation function predicted by our description for temperatures below 2000 K (Fig. 18) accounts well for the estimates by Brewer and Wenger [124], which were not used in the present evaluation.

### 6.2.2. Metastable carbides

Part of the present work focused on the estimation of thermodynamic values for metastable compounds. In particular, by combining the methods described in

Section 5 with the optimization technique, and by performing systematic calculations of the Zr–C phase diagram, it was possible to obtain the Gibbs energy functions of two metastable carbides which are involved in the CEM [45,46] for the interstitial phases in this system, i.e. the  $ZrC_{0.5}$  and  $ZrC_3$  carbides. Thus it is interesting to compare these results with the predictions of other approaches to thermochemical values for metastable compounds. In particular, we shall compare the present enthalpy of formation values at 298.15 K with the values given by the method developed by Miedema and coworkers [114]. Such a comparison is given in Fig. 19, where we plot the enthalpy of formation values for various Zr carbides vs. the atomic fraction of carbon in the compound. The present estimates for  $ZrC_{0.5}$  and the experimental value for the stoichiometric ZrC phase

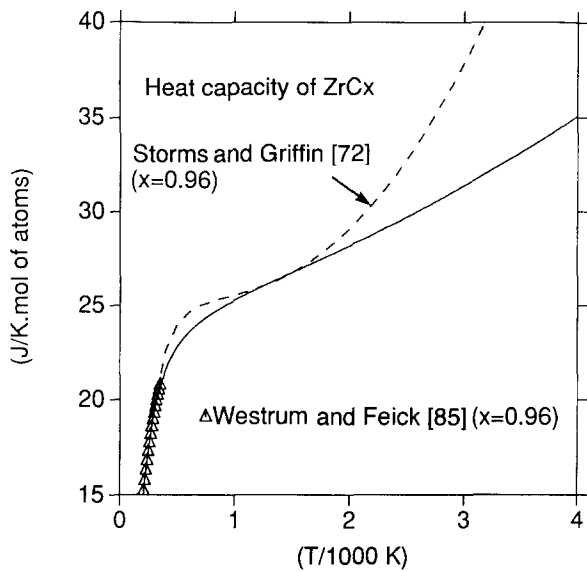


Fig. 11. The calculated heat capacity of the  $ZrC_{0.96}$  carbide as a function of temperature (—) compared with experimental data (symbols) and the values recommended by Storms and Griffin [72] (---).

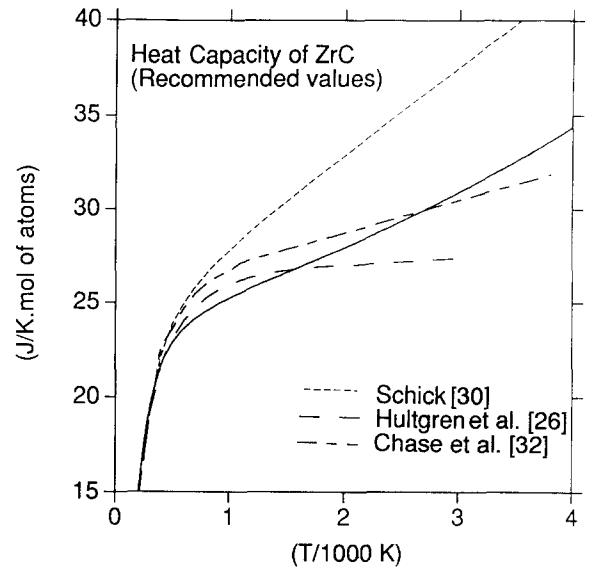


Fig. 13. The calculated heat capacity of the ZrC carbide as a function of temperature (—) compared with the values recommended by Schick [30] and Hultgren et al. [26] and in the JANAF thermochemical tables [32].

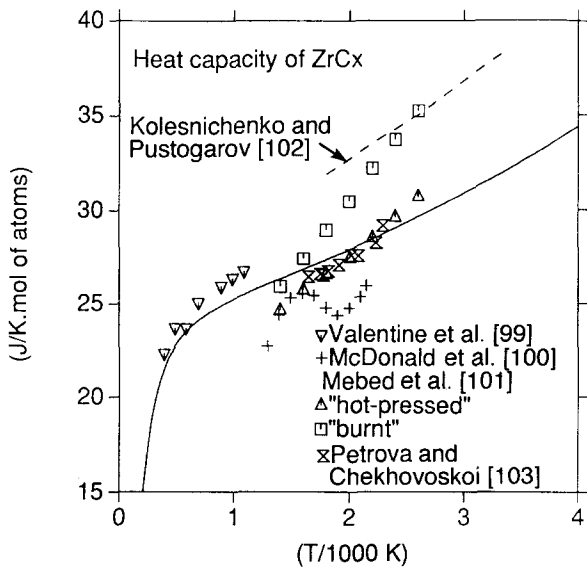


Fig. 12. The calculated heat capacity of the ZrC carbide as a function of temperature (—) compared with experimental data (symbols). ---, experimental results by Kolesnichenko and Pustogarov [102].

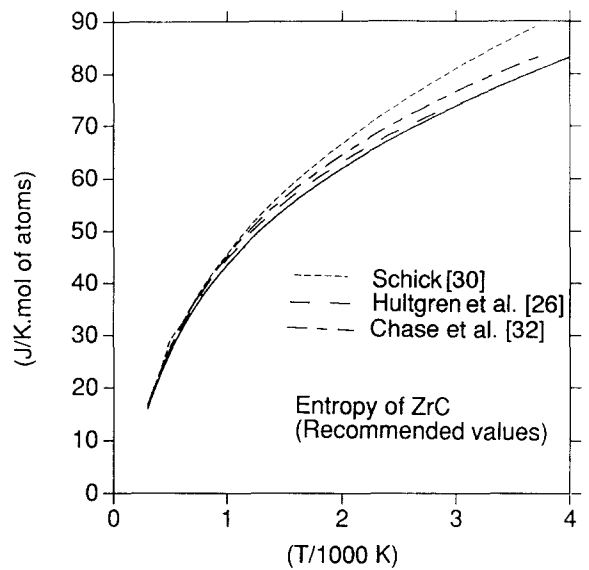


Fig. 14. The calculated entropy of the ZrC carbide as a function of temperature (—) compared with the values recommended by Schick [30] and Hultgren et al. [26] and in the JANAF thermochemical tables [32].

are in excellent agreement with the values from Miedema's formula [114], but there is a significant discrepancy for  $ZrC_3$ . In fact, calculations of the Zr–C phase diagram based on adopting for  $ZrC_3$  the enthalpy of formation predicted by Miedema and coworkers [114], i.e.  $-54 \text{ kJ (mol atoms)}^{-1}$ , together with the entropy function obtained in Section 5.3, led to the  $ZrC_3$  phase becoming stable in the Zr–C phase diagram, which is against experiments. As a consequence, the enthalpy value preferred by us,  $-25 \pm 25 \text{ kJ (mol atoms)}^{-1}$ , is less negative. Still, the general trend in the variation in the enthalpy of formation of Zr carbides

with the carbon content is compatible with the predictions of Miedema and coworkers [114].

### 7. Summary and concluding remarks

The thermochemical properties and the stability of the condensed phases in the Zr–C system have been the subject of numerous experimental studies. In addition, various reviews have been presented which aimed at compiling and critically analysing the data, and

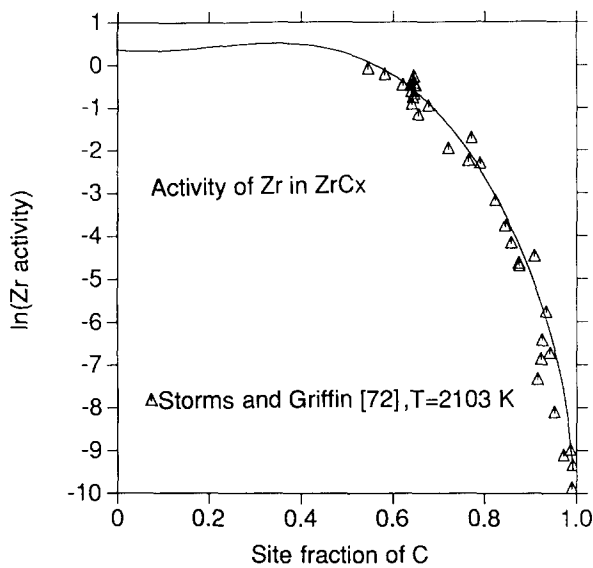


Fig. 15. The activity of Zr in the  $ZrC_x$  carbide at 2103 K as a function of the fraction of C atoms in its sublattice (—) compared with experimental data (symbols).

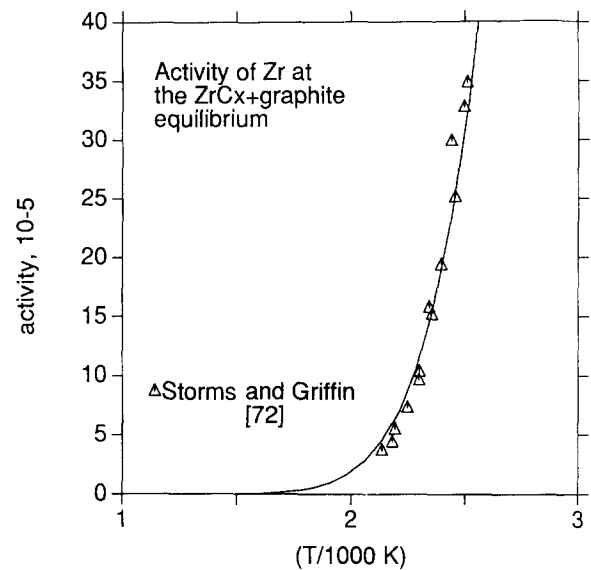


Fig. 17. The activity of Zr in the  $ZrC_x$  carbide in equilibrium with graphite as a function of temperature (—) compared with experimental data (symbols).

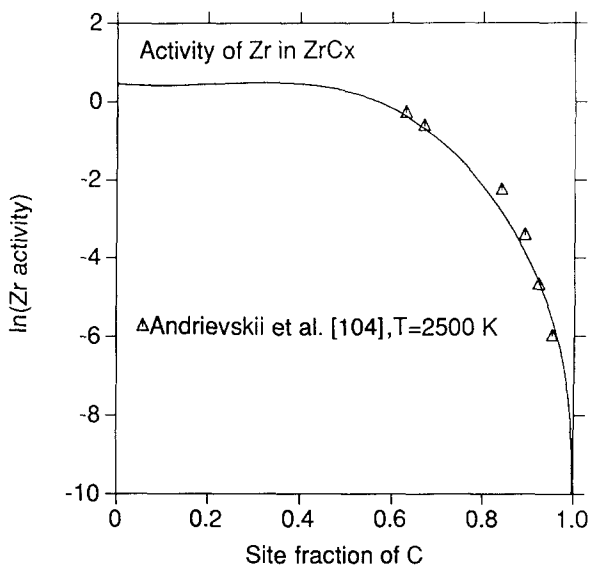


Fig. 16. The calculated activity of Zr in the  $ZrC_x$  carbide at 2500 K as a function of the fraction of C atoms in its sublattice (—) compared with experimental data (symbols).

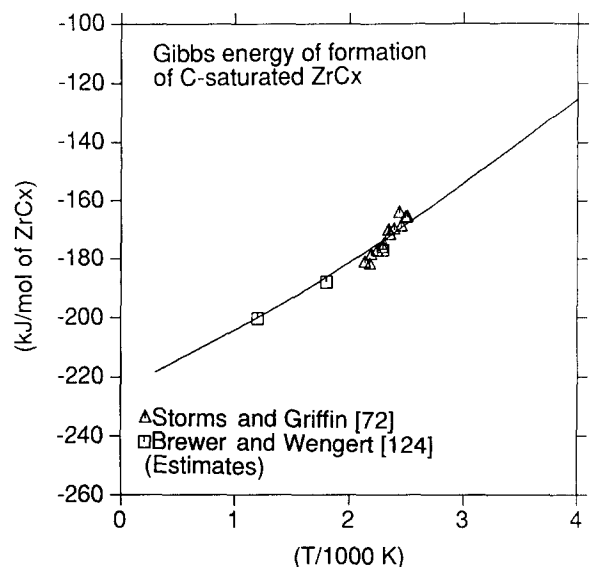


Fig. 18. The Gibbs energy of formation of the  $ZrC_x$  carbide saturated with graphite as a function of temperature (—) compared with experimental data by Storms and Griffin [72] and with estimates by Brewer and Wengert [124] (symbols).

producing a reliable description of the thermodynamics of the system. However, these analyses often focused on a certain kind of information, e.g. on the phase diagram, without making use of the relation between the phase diagram and the thermochemical properties of the individual phases. In addition, the information available has not been complete, and thus those various attempts to produce a complete picture of the Zr–C system have been forced to rely on extrapolations of the measured values and estimation of lacking data. In general this led to significant discrepancies between the expected values for some quantities in the system, such as the thermodynamic properties of the  $ZrC_x$  phase

at very high temperatures. The assessment procedure applied in the present work is based on the use of mathematical models for the Gibbs energy functions of the various phases in the system, from which both the phase diagram and the thermochemical properties can be calculated. This guarantees the thermodynamic consistency of the results. In addition, the parameters in the models have been evaluated by applying a computer optimization technique that allows the various kinds of selected data to be treated at the same time. In this way, both thermochemical measurements and phase diagram information are allowed to influence

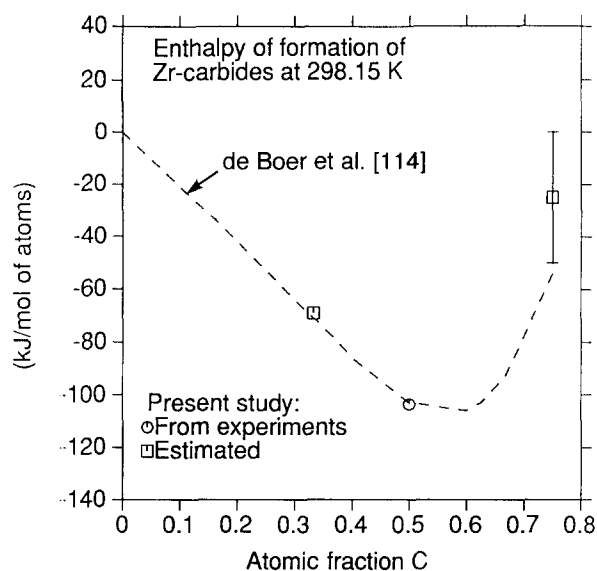


Fig. 19. The enthalpy formation of  $ZrC_{0.5}$ ,  $ZrC$  and  $ZrC_3$  at 298.15 K as a function of the atomic fraction of C, according to the present study (symbols) compared with the values predicted by the Miedema approach [114] (---).

the values for Gibbs energy. Therefore, the phase diagram calculated using the optimum thermodynamic parameters is expected to be more reliable than those obtained by using methods of interpolation (e.g. graphical) that cannot take into account the thermochemical properties of the individual phases. The picture of the thermodynamics of the Zr–C system that emerges from the present analysis is of a general compatibility between experiments and model calculations, but some significant discrepancies are found. In addition, the systematization of the available information that has been performed as a part of this work reveals a lack of experimental data on certain properties or regions of the system. New thermodynamic measurements, in particular on the liquid phase, would help to refine the present description. Finally, the present assessment has involved the application of a procedure for estimating thermodynamic properties for metastable compounds, and the comparison with the predictions of the method by Miedema and coworkers [114]. As in other metal–carbon [18,19,107], metal–nitrogen [19,115,116,125–127] and metal–metal [128] systems of the transition series we found a qualitative agreement with the trends in Miedema and coworkers' [114] values, but significant quantitative discrepancies are detected.

### Acknowledgment

This work is part of a research project supported by the Consejo Nacional de Investigaciones Científicas y Técnicas of Argentina, under Grant PIA-0028/92.

### References

- [1] L. Kaufman and H. Bernstein, *Computer Calculation of Phase Diagrams*, Academic Press, New York, 1970.
- [2] T.B. Massalski, H. Okamoto, P.R. Subramanian and L. Kacprzak, *Binary Alloy Phase Diagrams*, American Society for Metals International, Metals Park, OH, 2nd edn., 1990.
- [3] K. Balasubramanian, Division of Physical Metallurgy, The Royal Institute of Technology, Stockholm, Sweden, unpublished research.
- [4] W. Huang, *Z. Metallkd.*, 82 (1991) 174–181.
- [5] J.-O. Andersson, *CALPHAD*, 11 (1987) 271–276.
- [6] W. Huang, *Scand. J. Metall.*, 19 (1990) 26–32.
- [7] P. Gustafson, *Scand. J. Metall.*, 14 (1985) 259–267.
- [8] A. Fernández Guillermet, *Z. Metallkd.*, 78 (1987) 700–709.
- [9] P. Gustafson, A. Gabriel and I. Ansara, *Z. Metallkd.*, 78 (1987) 151–156.
- [10] W. Huang, *Mater. Sci. Technol.*, 6 (1990) 687–694.
- [11] J.-O. Andersson, *CALPHAD*, 12 (1988) 1–8.
- [12] P. Gustafson, *Mater. Sci. Technol.*, 2 (1986) 653–658.
- [13] J.-O. Andersson, *Ph.D. Thesis*, Division of Physical Metallurgy, The Royal Institute of Technology, Stockholm, Sweden, 1986.
- [14] W. Huang, *Ph.D. Thesis*, Division of Physical Metallurgy, The Royal Institute of Technology, Stockholm, Sweden, 1990.
- [15] P. Gustafson, *Ph.D. Thesis*, Division of Physical Metallurgy, The Royal Institute of Technology, Stockholm, Sweden, 1987.
- [16] A. Fernández Guillermet, *Z. Metallkd.*, 80 (1989) 83–94.
- [17] A. Fernández Guillermet and G. Grimvall, *Phys. Rev. B*, 40 (1989) 10582–10593.
- [18] A. Fernández Guillermet and G. Grimvall, *J. Phys. Chem. Solids*, 53 (1992) 105–125.
- [19] A. Fernández Guillermet, J. Häglund and G. Grimvall, *Phys. Rev. B*, 45 (1992) 11557–11567.
- [20] A. Fernández Guillermet, J. Häglund and G. Grimvall, *Phys. Rev. B*, 48 (1993) 11673–11684.
- [21] E.T. Hayes, in B. Lustman and F. Kerze, Jr., (eds.), *The Metallurgy of Zirconium*, McGraw-Hill, New York, 1955.
- [22] M. Hansen and K. Anderko, *Constitution of Binary Alloys*, McGraw-Hill, New York, 1958.
- [23] R.P. Elliott, *Constitution of Binary Alloys, First Supplement*, McGraw-Hill, New York, 1965.
- [24] E.K. Storms, *The Refractory Carbides*, Academic Press, New York, 1967.
- [25] F.A. Shunk, *Constitution of Binary Alloys, Second Supplement*, McGraw-Hill, New York, 1969.
- [26] R. Hultgren, P.D. Desai, D.T. Hawkins, M. Gleiser, K.K. Kelley and D.D. Wagman, *Selected Values of the Thermodynamic Properties of Binary Alloys*, American Society for Metals, Metals Park, OH, 1973.
- [27] O. Kubaschewski-von Goldbeck, in O. Kubaschewski (ed.), *Zirconium: Physico-Chemical Properties of its Compounds and Alloys*, in *Atomic Energy Review*, Special Issue 6, International Atomic Energy Agency, Vienna, 1976.
- [28] H. Okamoto, in Ref. [2], pp. 899–900.
- [29] O. Kubaschewski and J.A. Catterall, *Thermochemical Data of Alloys*, Pergamon, London, 1956.
- [30] H.L. Schick, *Thermodynamics of Certain Refractory Compounds*, Vols. I and II, Academic Press, New York, 1966.
- [31] C.B. Alcock, K.T. Jakob and S. Zador, in O. Kubaschewski (ed.), *Zirconium: Physico-Chemical Properties of its Compounds and Alloys*, in *Atomic Energy Review*, Special Issue 6, International Atomic Energy Agency, Vienna, 1976.
- [32] M.W. Chase, C.A. Davies, J.R. Downey, Jr., D.J. Frurip, R.A. McDonald and A.N. Syverud, *JANAF Thermochemical Tables*, 3rd edn., in *J. Phys. Chem. Ref. Data*, 14 (Suppl. 1) (1985).
- [33] G.L. De Poorter, *J. Am. Ceram. Soc.*, 52 (1969) 311–315.

- [34] M. Hoch, in P.S. Rudman, J. Stringer and R.I. Jaffee (eds.), *Phase Stability of Metals and Alloys*, McGraw-Hill, New York, 1967.
- [35] V.N. Zagryazkin, A.S. Panov and E.V. Fiveiskii, in *Thermodynamics of Nuclear Materials, Proc., 1974*, Vol. 2, pp. 431–437.
- [36] L. Kaufman and A. Sarney, in J.T. Waber, P. Chiotti and W.N. Miner (eds.), *Proc. Int. Symp. on Compounds of Interest in Nuclear Reactor Technology*, Metallurgical Society of AIME, Ann Arbor, MI, 1964, pp. 267–278.
- [37] Y.A. Chang, *Tech. Rep. AFML-TR-65-2*, Part IV, Vol. I, 1965 (Air Force Materials Laboratory, Research and Technology Division, Air Force Systems Command, Wright-Patterson Air Force Base, OH). (Cited in Ref. [72].)
- [38] L. Kaufman and E.V. Clougherty, in *Metallurgy at High Temperatures and Pressures*, Metallurgical Society of AIME Conferences, Vol. 22, Gordon and Breach, New York, 1964, pp. 322–380.
- [39] A. Fernández Guillermet, *High Temp. High Pressures*, 19 (1987) 119–160.
- [40] N. Saunders, A.P. Miodownik and A.T. Dinsdale, *CALPHAD*, 12 (1988) 351–374.
- [41] P. Gustafson, *Carbon*, 24 (1986) 169–176.
- [42] G. Hägg, *Z. Phys. Chem. B*, 12 (1931) 33–56.
- [43] H.J. Goldschmidt, *Interstitial Alloys*, Butterworth, London, 1967.
- [44] L.E. Toth, *Transition Metal Carbides and Nitrides*, Academic Press, New York, 1971.
- [45] J.-O. Andersson, A. Fernández Guillermet, M. Hillert, B. Jansson and B. Sundman, *Acta Metall.*, 34 (1986) 437–445.
- [46] M. Hillert and L.-I. Staffansson, *Acta Chem. Scand.*, 24 (1970) 3618–3626.
- [47] B. Sundman and J. Ågren, *J. Phys. Chem. Solids*, 42 (1981) 297–301.
- [48] M. Hillert, in L.H. Bennett (ed.), *Computer Modeling of Phase Diagrams*, Metallurgical Society, Warrendale, PA, 1986, pp. 1–17.
- [49] O. Redlich and A.T. Kister, *Ind. Eng. Chem.*, 40 (1948) 345–348.
- [50] H. Ohtani and M. Hillert, *CALPHAD*, 14 (1990) 289–306.
- [51] A. Fernández Guillermet and S. Jonsson, *Z. Metallkd.*, 83 (1992) 21–31.
- [52] B. Jansson, *Ph.D. Thesis*, Division of Physical Metallurgy, The Royal Institute of Technology, Stockholm, Sweden, 1984.
- [53] E. Friederich and L. Sitting, *Z. Anorg. Chem.*, 144 (1925) 169–189.
- [54] C. Agte and H. Alterthum, *Z. Tech. Phys.*, 11 (1930) 182–191.
- [55] F.W. Glaser. (Value quoted by P. Schwarzkopf and R. Kieffer, *Refractory Hard Metals*, Macmillan, New York, 1953.)
- [56] L.D. Brownlee, *J. Inst. Met.*, 87 (1958–1959) 58–61.
- [57] J. Farr, unpublished work. (Cited by E.K. Storms, *LAMS-2674*, 1962.)
- [58] V.N. Paderno, *Russ. Met. Fuels*, 6 (1962) 104. (Cited in Ref. [25].)
- [59] R.V. Sara, *J. Am. Ceram. Soc.*, 48 (1965) 243–247.
- [60] E. Rudy, D.P. Harmon and C.E. Brukl, *Tech. Rep. AFML-TR-65-2*, Part I, Vol. II, 1965 (Air Force Materials Laboratory, Research and Technology Division, Air Force Systems Command, Wright-Patterson Air Force Base, OH).
- [61] E. Rudy and J. Progulski, *Planseeber. Pulvermetall.*, 15 (1967) 13–45.
- [62] E. Rudy, *Tech. Rep. AFML-TR-65-2*, Part V, 1969 (Air Force Materials Laboratory, Research and Technology Division, Air Force Systems Command, Wright-Patterson Air Force Base, OH).
- [63] Yu.P. Zotov and R.V. Kotelnikov, *Izv. Akad. Nauk SSSR, Met.*, 1 (1975) 179–181.
- [64] L.M. Adelsberg, L.H. Cadoff and J.M. Tobin, *Trans. AIME*, 236 (1966) 972–977.
- [65] C. Agte and K. Moers, *Z. Anorg. Chem.*, 198 (1931) 248. (Cited in Ref. [60].)
- [66] P. Chiotti and L. Weiner, Iowa State College, personal communications to E.T. Hayes, January 1954. (Cited in Ref. [21].)
- [67] K.I. Portnoi, Yu.V. Levinskii and V.I. Fadeeva, *Izv. Akad. Nauk SSSR, Otd. Tekh. Nauk, Met. Topl.*, 2 (1961) 147–149. (Cited in Ref. [60].)
- [68] T.C. Wallace, C.P. Gutierrez and P.L. Stone, *J. Phys. Chem.*, 67 (1963) 796–801.
- [69] L.M. Adelsberg, L.H. Cadoff and J.M. Tobin, *J. Am. Ceram. Soc.*, 49 (1966) 573–574.
- [70] F. Benesovsky and E. Rudy, *Planseeber. Pulvermetall.*, 8 (1960) 66–71.
- [71] Y.J. Bhatt, R. Venkataramani and S.P. Garg, *J. Less-Common Met.*, 132 (1987) L21–L24.
- [72] E.K. Storms and J. Griffin, *High Temp. Sci.*, 5 (1973) 291–310.
- [73] Yu. G. Godin, A.I. Evstyukhin, A.I. Emel'yanov, A.A. Rusakov and I.I. Suchkov, *Metall. Metalloved. Chistykh Met., Sb. Nauchn. Rab.*, 3 (1961) 284–289.
- [74] V.M. Anan'in, V.P. Gladkov, V.S. Zotov and D.M. Skorov, *Obshch. Zakonomern. Str. Diag. Sostoy. Met. Sist., Mater. Vses. Soveshch.*, 5th (1973) 45–46.
- [75] G.L. Humphrey, *J. Am. Chem. Soc.*, 76 (1954) 978–980.
- [76] E.J. Huber, Jr., E.L. Head and C.E. Holley, Jr., *J. Phys. Chem.*, 68 (1964) 3040–3042.
- [77] A.D. Mah and B.J. Boyle, *J. Am. Chem. Soc.*, 77 (1955) 6512–6513.
- [78] A.D. Mah, *US Bureau of Mines Report of Investigations 6518*, US Department of the Interior, 1964.
- [79] F.B. Baker, E.K. Storms and C.E. Holley, Jr., *J. Chem. Eng. Data*, 14 (1969) 244–246.
- [80] O. Kubaschewski and C.B. Alcock, *Metallurgical Thermochemistry*, Pergamon, Oxford, 5th edn., 1983.
- [81] A.N. Kornilov, N.V. Chelovskaya and V.I. Zhelankin, *Russ. J. Phys. Chem.*, 49 (1975) 792.
- [82] V.M. Maslov, A.S. Neganov, I.P. Borovinskaya and A.G. Merzhanov, *Fiz. Goreniya Vzryva*, 14 (1978) 73–82.
- [83] B.D. Pollock, *J. Phys. Chem.*, 65 (1961) 731–735.
- [84] J.A. Coffman, G.M. Kibler, T.F. Lyon and B.D. Accchione, *Tech. Rep., WADD-TR-60-646*, Part II, 1963 (Wright-Patterson Air Force Base).
- [85] E.F. Westrum, Jr., and G. Feick, *J. Chem. Eng. Data*, 8 (1963) 176–178.
- [86] D.S. Neel, C.D. Pears and S. Oglesby, Jr., research performed by the Southern Research Institute, *Tech. Rep. WADD-TR-60-924*, 1962 (Air Force Systems Command, Wright Patterson Air Force Base, OH).
- [87] R. Mezaki, T.F. Jambois, A.K. Gangopadhyay and J.L. Margrave, in L.A. McClaine (ed.), *Thermodynamic and Kinetic Studies for a Refractory Materials Program, Tech. Rep. ASD-TDR-62-204*, Part II, 1963 (Air Force Materials Laboratory, Aeronautical Systems Division, Air Force Systems Command, Wright-Patterson Air Force Base, OH).
- [88] R. Mezaki, E.W. Tilleux, T.F. Jambois and J.L. Margrave, in *3rd Symp. on Thermophysical Properties, Lafayette, 1965*, pp. 138–145.
- [89] L.S. Levinson, *J. Chem. Phys.*, 42 (1965) 2891–2892.
- [90] A.S. Bolgar, E.A. Guseva and V.V. Fesenko, *Poroshk. Metall.*, (No. 1) (49) (1967) 40–43.
- [91] P.B. Kantor and E.N. Fomichev, *Teplofiz. Vys. Temp.*, 5 (1967) 48–51.
- [92] A.G. Turchanin and V.A. Fesenko, *Poroshk. Metall.*, (No. 1) (61) (1968) 88–90.
- [93] A.G. Turchanin and V.V. Fesenko, *Poroshk. Metall.*, (No. 6) (78) (1968) 48–52.
- [94] A.G. Turchanin and V.V. Fesenko, *Heat Transfer Sov. Res.*, 5 (1973) 23–28.

- [95] V.V. Fesenko, A.G. Turchanin and S.S. Ordan'yan, in G.V. Samsonov (ed.), *Refractory Carbides*, Plenum, New York, 1974, pp. 323–328.
- [96] A.G. Turchanin, *Izv. Akad. Nauk SSSR, Neorg. Mater.*, 17 (1981) 262–264.
- [97] A.G. Turchanin, *Izv. Akad. Nauk SSSR, Neorg. Mater.*, 22 (1986) 1299–1302.
- [98] A.E. Sheindlin, V. Ya. Chekovskoi and E.E. Shpil'rain, *High Temp. High Pressures*, 2 (1970) 1–15.
- [99] R.H. Valentine, T.F. Jambois and J.L. Margrave, personal communication to R.A. McDonald. (Values quoted in Ref. [100].)
- [100] R.A. McDonald, F.L. Oetting and H. Prophet, in *Proc. Meet. Interagency Chemical Rocket Propulsion, Group of Thermochemistry, New York, 1963, CPIA 44*, Vol. 1, Johns Hopkins University, Applied Physics Laboratory, Silver Spring, MD, 1954, pp. 213–245.
- [101] M.M. Mebed, R.P. Yurchak and L.A. Korolev, *Teplofiz. Vys. Temp.*, 11 (1973) 427–429.
- [102] A.P. Kolesnichenko and A.V. Pustogarov, *Teplofiz. Vys. Temp.*, 13 (1975) 1197–1201.
- [103] I.I. Petrova and V.Ya. Chekhovskoi, *Teplofiz. Vys. Temp.*, 16 (1978) 1226–1231.
- [104] R.A. Andrievskii, V.V. Khromonozhkin, Yu.F. Khromov, I.S. Alekseeva and V.A. Mitrokhin, *Dokl. Akad. Nauk SSSR*, 206 (1972) 896–898.
- [105] A. Fernández Guillermet and G. Grimvall, *Z. Metallkd.*, 81 (1990) 521–524.
- [106] A. Fernández Guillermet, *Int. J. Thermophys.*, 12 (1991) 919–936.
- [107] A. Fernández Guillermet and W. Huang, *Int. J. Thermophys.*, 12 (1991) 1077–1102.
- [108] G. Grimvall and A. Fernández Guillermet, in S.K. Saxena (ed.), *Thermodynamic Data, Systematics and Estimation*, Advances in Physical Geochemistry, Vol. 10, Springer, New York, 1992, pp. 270–282.
- [109] G. Grimvall, *Thermophysical Properties of Materials*, North-Holland, Amsterdam, 1986.
- [110] G. Grimvall and J. Rosén, *Int. J. Thermophys.*, 4 (1983) 139–147.
- [111] A. Fernández Guillermet and G. Grimvall, *Phys. Rev. B*, 40 (1989) 1521–1527.
- [112] A. Fernández Guillermet and G. Grimvall, *J. Less-Common Met.*, 69 (1991) 257–281.
- [113] G. Grimvall and A. Fernández Guillermet, in D. Emin, T.L. Aselage, A.C. Switendick, B. Morosin and C.L. Beckel (eds.), *Boron-Rich Solids, Albuquerque, NM 1990*, in *AIP Conf. Proc.*, 231 (1991) 423–430.
- [114] F.R. de Boer, R. Boom, W.C. Mattens, A.R. Miedema and A.K. Niessen, *Cohesion in Metals, Transition Metal Alloys*, North-Holland, Amsterdam, 1988.
- [115] A. Fernández Guillermet and S. Jonsson, *Z. Metallkd.*, 84 (1993) 106–117.
- [116] A. Fernández Guillermet and K. Frisk, in *CALPHAD XXI, Jerusalem, June 14–19, 1992*, to be published.
- [117] B. Sundman, B. Jansson and J.-O. Andersson, *CALPHAD*, 9 (1985) 153–190.
- [118] B. Jönsson and B. Sundman, *High Temp. Sci.*, 26 (1988–1989) 263–273.
- [119] Yu.N. Vil'k, S.S. Ordan'yan, R.G. Avarbe, A.I. Avgustinik, T.P. Ryzhkova and Yu.A. Omel'chenko, *J. Appl. Chem. USSR*, 38 (1965) 1472–1476.
- [120] H.A. Wilhelm, C.B. Hamilton and K.M. Wolf, *US Atomic Energy Commun., IS-900*, 1964, pp. M45–M46. (Cited in Ref. [25].)
- [121] E.G. Kendall, J.I. Slaughter and W.C. Riley, *Reps. A65-23321 and SSD-TR-65-78*, 1965 (Ballistic Systems and Space Systems Division, Air Force Systems Command, Los Angeles Air Force Station, Los Angeles, CA). (Cited in Ref. [24].)
- [122] H. Nickel, Ö. Inane and K. Lucke, *Z. Metallkd.*, 59 (1968) 935–940.
- [123] G.L. Vidale, *Tech. Inf. Ser. R61SD147*, 1961 (Space Sciences Laboratory, General Electric Co., King of Prussia, PA). (Cited in Ref. [24].)
- [124] L. Brewer and P.R. Wengert, *Metall. Trans.*, 4 (1973) 83–104.
- [125] C. Qiu and A. Fernández Guillermet, *Z. Metallkd.*, 84 (1993) 11–22.
- [126] A. Fernández Guillermet and H. Du, *Z. Metallkd.*, 85 (1994) 154–163.
- [127] A. Fernández Guillermet and K. Frisk, *J. Alloys Comp.*, 203 (1994) 77–89.
- [128] A. Fernández Guillermet, *Z. Metallkd.*, 82 (1991) 478–487.